Mechanical Influence of the Intervertebral Disc on the Vertebrae

A Finite Element Analysis

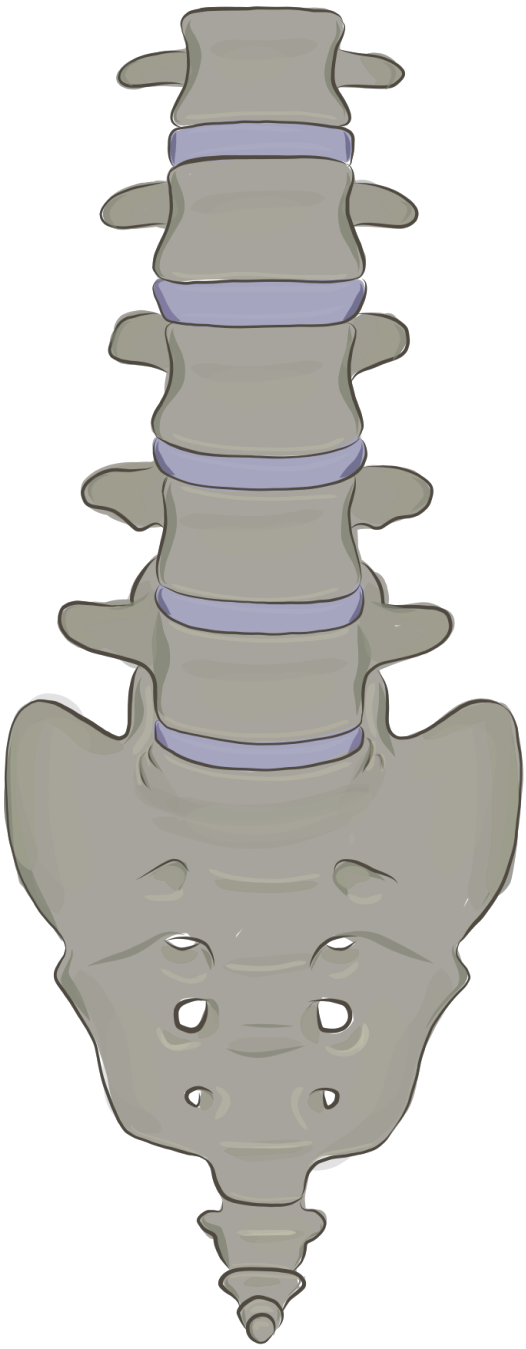

Eliane Tazelaar

Delft University of Technology
Imperial College London

April 2019

Mechanical Influence of the Intervertebral Disc on the Vertebrae

A Finite Element Analysis

By

Eliane Tazelaar

A thesis submitted in partial fulfilment of the requirements for the degree of

Master of Science

in Biomedical Engineering

Delft University of Technology
To be defended on April 15th, 2019

Supervision: Prof. dr J. Dankelman, Delft University of Technology
Dr. A. Phillips, Imperial College London
C. Favier Imperial College London

An electronic version of this dissertation is available at
http://repository.tudelft.nl/.

Imperial College London

TU Delft Delft University of Technology

CONTENTS

ACRONYMS

FEM Finite Element Method 1
FEA Finite Element Analysis ix
FE Finite Element ix
LBP Low Back Pain 1
NP Nucleus Pulposus ix
AF Anulus Fibrosus ix
CEPS Cartilage End Plates 1
BEPS Bony End Plates 1

LIST OF FIGURES

LIST OF TABLES

ABSTRACT

Background: To find treatment options for lower back pain, one must gain insight in the spinal anatomy and biomechanics such as joint reaction forces and movement strategies. These can be acquired with use of the Finite Element Method. Previously investigated finite element models of the lumbar intervertebral disc have been designed with the main purpose of understanding the biomechanics of the disc itself, and not necessarily its influence on other spinal elements. A change in disc biomechanics is hypothesised to cause a disruption in the surrounding structures such as the vertebrae which, in turn, could result in lower back pain.

Goal: To create a finite element model of a spinal unit for investigating mechanical influences of the disc onto its adjacent vertebrae. Assessment was performed by examining bone adaptation as a result from simulated disc generation.

Methods: A `MATLAB` script was written to assemble an input file of a parametric model to be used for finite element analyses in `Abaqus/CAE`. The model was validated with experimental data from literature. A bone adaptation algorithm was used to assess a change in bone material properties before and after simulating disc degeneration by adjusting disc material properties.

Results: Finite element analyses showed how a load was transferred by the disc and how bone consequently adapted in response to simulated disc degeneration. The overall trabecular structure was observed to become softer, especially in the vertebral core, while the structure inferior to the anulus became relatively stiffer.

Conclusions: Visualisation of bone adaptation after simulating disc degeneration supports the hypothesis that disrupted disc biomechanics indeed affect bone configuration in adjacent vertebrae.

1

General Introduction

This is a report on a research project investigating the influence of the human lumbar intervertebral disc on its adjacent vertebrae with the use of the Finite Element Method (FEM). Additionally, a scientific article was written and is attached to the end of this report. The project was carried out at the Department of Civil & Environmental Engineering of Imperial College London under supervision of dr. Andrew Phillips and Clément Favier of the Structural Biomechanics Research Group. It was submitted to professor Jenny Dankelman as supervisor from the Delft University of Technology in partial fulfillment of the requirements for the degree of Master of Science in Biomedical Engineering.

1.1. Background

The human spine consists of various parts. All are connected in one or more ways and together, they form a flexible, curved vertebral column enabling the human body to move and stand upright by providing axial support and transmitting loads [1]. It is divided in five sections that are each distinct by different types of vertebrae. The lower back is supported by the biggest five, the lumbar vertebrae. Figure 1.1(a) shows a median sagittal section of a part of the lumbar back. The intervertebral discs (Figure 1.1(b)) separate the vertebrae and function as load distributing and shock absorbing pads. They function as a joint and allow the vertebrae to move relative to each other resulting in flexion, extension and bending of the spine [2]. They are tightly connected to the vertebrae through the end plates, which in turn, consist of Cartilage End Plates (CEPS) and Bony End Plates (BEPS). Numerous muscles and ligaments provide muscle force for these motions and at the same time prevent the vertebrae and discs from translational movements [3]. A vertebral joint is also known as a spinal unit and consists of one disc, its two adjacent end plates and vertebrae and ligaments.

Low Back Pain (LBP) has been defined as "pain and discomfort, localised below the costal margin and above the inferior gluteal folds, with or without leg pain" [4]. The high number and variety in elements of the spine make it difficult to define a main cause for LBP.

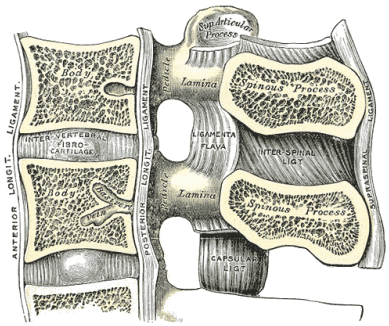

(a) Median sagittal section of two lumbar vertebrae, two intervertebral discs and five ligaments. Taken from Gray and Lewis [13].

(b) Median sagittal section of the intervertebral disc and its components. Taken from Neumann [14], which was modified from Bogduk [2]

Figure 1.1: Two median sagittal sections of a part of the lumbar spine.

In pursuit of finding treatment options, however, one must gain insight in the spinal anatomy and biomechanics such as joint reaction forces and movement strategies. Various studies on spinal anatomy and biomechanics hypothesise about (potential) causes of pain. Toyone *et al.* [5] carried out MRI studies to investigate correlations between altered vertebral bone-marrow as a result of degenerative intervertebral disc and LBP. Lotz *et al.* [6] write that degenerating discs are often cause of *annulogenic* pain resulting in LBP [7, 8]. Nevertheless, they state that studies by Fagan *et al.* [9] investigating innervation of the end plates give evidence that damaged end plates causing *vertebrogenic* pain could also be a major source of LBP. Zhao *et al.* [10] performed experiments to assess vertebral fractures in end plates and found that in case of failure, this often occurs in cranial BEPS before caudal BEPS. Several studies report that vertebral microfractures can be a source of back pain [11, 12].

1.2. MOTIVATION

To gain insight in potential causes of LBP, it is important to comprehend how various anatomical structures influence each other. Disruption in the intervertebral disc is often mentioned as a potential cause of LBP [15]. A direct cause can be i.e. "sensitized nociceptors within the annulus fibrosus of degenerating disks" [6]. *In vivo* and *in vitro* experiments have provided a great amount of information but they are unsuitable to assess internal stress and strain or fluid and solute exchange [16]. Schmidt *et al.* [16] write that several FE studies on intervertebral discs have proven the FEM to be a decent method to assess disc functioning.

1.3. PROBLEM STATEMENT

Previously investigated FE models of the lumbar intervertebral disc have been designed with the main purpose of understanding the biomechanics of the disc itself, and not necessarily its influence on to other spinal elements. It is, however, hypothesised that a change in disc biomechanics could cause a disruption in the surrounding structures,

more specifically the vertebrae. Subsequently, vertebral disruption could induce weakening of the bone structure, making the vertebrae and end plates more prone to (micro)fracturing which, in turn, could result in LBP.

Consequently, the following research question arises:

> *What is the mechanical influence of the intervertebral disc on its adjacent vertebrae?*

1.4. RESEARCH OBJECTIVES

This project was set up to acquire scientific insight in the biomechanics of the lower spine. To help ensuring that a complete overview is provided, five research objectives were formulated:

1. *To build a finite element model of a spinal unit.*
2. *To comment on the validity of the model.*
3. *To gain insight in load transmission and the process of bone adaptation as result of disrupted disc biomechanics.*
4. *To approach answering this project's research question supported by FEA results.*
5. *To reflect upon this project's relevance for research in LBP.*

1.5. THESIS OUTLINE

This report consists of four substantive chapters:

- **Chapter 2**: Background: Lumbar Anatomy elaborates on the anatomical background of this project.
- **Chapter 3**: Finite Element Model is a description of the modelling process.
- **Chapter 4**: Finite Element Analysis offers the assessment of the created model and the outcomes of the analysis.
- **Chapter 5**: Conclusion summarises the project's findings and provides suggestions for further research.

1

REFERENCES

[1] E. N. Marieb and K. Hoehn, *Human anatomy & physiology* (Pearson Education, 2007).

[2] N. Bogduk, *Clinical and Radiological Anatomy of the Lumbar Spine E-Book* (Elsevier Health Sciences, 2012).

[3] M. A. Adams and P. J. Roughley, *What is intervertebral disc degeneration, and what causes it?* Spine **31**, 2151 (2006).

[4] M. Van Tulder, A. Becker, T. Bekkering, A. Breen, M. T. Gil del Real, A. Hutchinson, B. Koes, E. Laerum, and A. Malmivaara, *Chapter 3 european guidelines for the management of acute nonspecific low back pain in primary care,* European spine journal **15**, s169 (2006).

[5] T. Toyone, K. Takahashi, H. Kitahara, M. Yamagata, M. Murakami, and H. Moriya, *Vertebral bone-marrow changes in degenerative lumbar disc disease. an mri study of 74 patients with low back pain,* The Journal of bone and joint surgery. British volume **76**, 757 (1994).

[6] J. Lotz, A. Fields, and E. Liebenberg, *The role of the vertebral end plate in low back pain,* Global spine journal **3**, 153 (2013).

[7] M. A. Adams and P. Dolan, *Intervertebral disc degeneration: evidence for two distinct phenotypes,* Journal of anatomy **221**, 497 (2012).

[8] K. Luoma, H. Riihimäki, R. Luukkonen, R. Raininko, E. Viikari-Juntura, and A. Lamminen, *Low back pain in relation to lumbar disc degeneration,* Spine **25**, 487 (2000).

[9] A. Fagan, R. Moore, B. V. Roberts, P. Blumbergs, and R. Fraser, *Issls prize winner: the innervation of the intervertebral disc: a quantitative analysis,* Spine **28**, 2570 (2003).

[10] F.-D. Zhao, P. Pollintine, B. Hole, M. Adams, and P. Dolan, *Vertebral fractures usually affect the cranial endplate because it is thinner and supported by less-dense trabecular bone,* Bone **44**, 372 (2009).

[11] F. Cecchi, P. Debolini, R. M. Lova, C. Macchi, S. Bandinelli, B. Bartali, F. Lauretani, E. Benvenuti, G. Hicks, and L. Ferrucci, *Epidemiology of back pain in a representative cohort of italian persons 65 years of age and older: the inchianti study,* Spine **31**, 1149 (2006).

[12] H. Sims-Williams, M. Jayson, and H. Baddeley, *Small spinal fractures in back pain patients.* Annals of the rheumatic diseases **37**, 262 (1978).

[13] H. Gray and W. Lewis, *Anatomy of the human body. 20th,* Philadelphia and New York, Lea & Febiger (1918).

[14] D. A. Neumann, *Kinesiology of the Musculoskeletal System-E-Book: Foundations for Rehabilitation* (Elsevier Health Sciences, 2013).

[15] N. Newell, J. Little, A. Christou, M. Adams, C. Adam, and S. Masouros, *Biomechanics of the human intervertebral disc: A review of testing techniques and results,* Journal of the mechanical behavior of biomedical materials **69**, 420 (2017).

[16] H. Schmidt, F. Galbusera, A. Rohlmann, and A. Shirazi-Adl, *What have we learned from finite element model studies of lumbar intervertebral discs in the past four decades?* Journal of biomechanics **46**, 2342 (2013).

2

BACKGROUND: LUMBAR ANATOMY

This chapter is an elaboration on the anatomical structures of the lower spine that are most important for this study. It provides insight in the material properties and mechanical composition of the elements and in how parts are relate to one another.

2.1. INTERVERTEBRAL DISC

The intervertebral disc is an element in the spinal column which main function is distributing loads by resisting spinal compression and simultaneously allowing the spine to bend and twist by permitting (limited) movements of the vertebrae with respect to each other [1]. The disc is composed of three main elements and fixed to the two adjacent vertebra through BEPS and CEPS. The gel like core, or NP, is encapsulated by the AF which is made up of ground matrix and collagen fibres. All elements are discussed in the following sections. Loads are uniformly spread through the end plates over the surface of the vertebrae, regardless of the angle between them, thus preventing damage as a result of high stress concentrations. Newell *et al.* [2] discusses studies showing that physical disruption such as changes in tissue properties of the disc can cause degeneration and consequently, altering of the disc's biomechanics [1, 3, 4]. Furthermore, correlations were found between disc degeneration and LBP [5, 6]. Adams *et al.* [7] describe functional changes as a consequence of disc degeneration. The NP decreases in size and consequently exerts less pressure on the AF. As a consequence, the latter has to provide more compressional load-bearing resistance. Simultaneously, the amount of proteoglycan in the AF decreases, reducing its compressional strength and increasing its stiffness [8].

2.1.1. NUCLEUS PULPOSUS

The NP is the core of the disc and takes up approximately 40-50% of an adult disc's total volume and 29% of the total cross sectional area [2]. It consists of cells and collagen type II dissolved in a water and proteoglycan solution. Proteoglycan gives the NP strong osmotic properties that cause the nucleus to swell or shrink by binding to or repelling

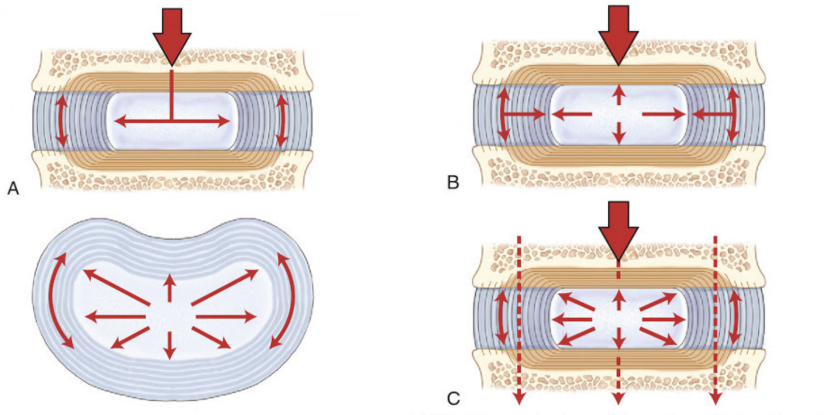

(a) Compressive force from body weight and muscle contraction leading to an increase in hydrostatic pressure in the NP and tensile forces in the AF.

(b) Increased tension in the AF inhibits radial expansion. Pressure is exerted both upwards as well as downwards and (c) Load is evenly distributed over the entire surface of the vertebral end plates.

Figure 2.1: The mechanism of force transmission through an intervertebral disc. Taken from Neumann [10], which was modified from Bogduk [11]

water, respectively. Swelling due to its high water content generates pressure on the AF and CEPS which, in turn, restrict swelling in all directions. This mechanism is the source of the disc's ability to withstand compressive forces [9] and is schematically depicted in Figures 2.1(a) and 2.1(b). To be able to fully understand the NP's functioning, it is important to understand its mechanical properties. However, testing the NP separate from the rest of the disc has proven to be rather difficult.

2.1.2. ANULUS FIBROSUS

The AF is an elastic ring, surrounding and confining the NP by restricting its outward-facing compressive forces resulting from hydrostatic pressure. It consists of several layers, lamellae, of soft ground matrix, that are enforced with strong fibre bundles. The ground matrix consists mostly of water and proteoglycans. The fibres are orientated at an angle of approximately 30 ° off horizontal and alternate direction per lamella. Neumann [10] explain that this specific orientation prevents torsion and vertical separation of the vertebrae while protecting the AF against shear stresses as a result from the tensile stresses that the NP imposes. Research has shown that the inner lamellae are generally more loosely arranged and consist of collagen type II and elastin fibres as opposed to the tightly layered outer lamellae that are enforced with collagen type I [1].

2.2. END PLATES

Literature is disagreeing on whether the end plates should be deemed part of the disc or of the vertebrae [12]. They are placed between the disc and the vertebral bodies and

formed by the CEPS and BEPS. They are described as a bilayer of hyaline cartilage and cortical bone and together, they are approximately 0.58 mm thick [2, 13, 14]. The bony component is found to be thicker in the lower vertebrae but there is a lack of quantitative data on the ratio between the two layers [12, 13, 15]. The two-component feature is clearly visible in Figure 2.2. Their main function is to balance the right trade-off between providing strength and porosity. On the one hand, they have to support the stiff vertebral bodies and protect them from fracturing and on the other hand, they allow for particle flow to and from the intervertebral disc. The latter is essential as the disc is not vascularised.

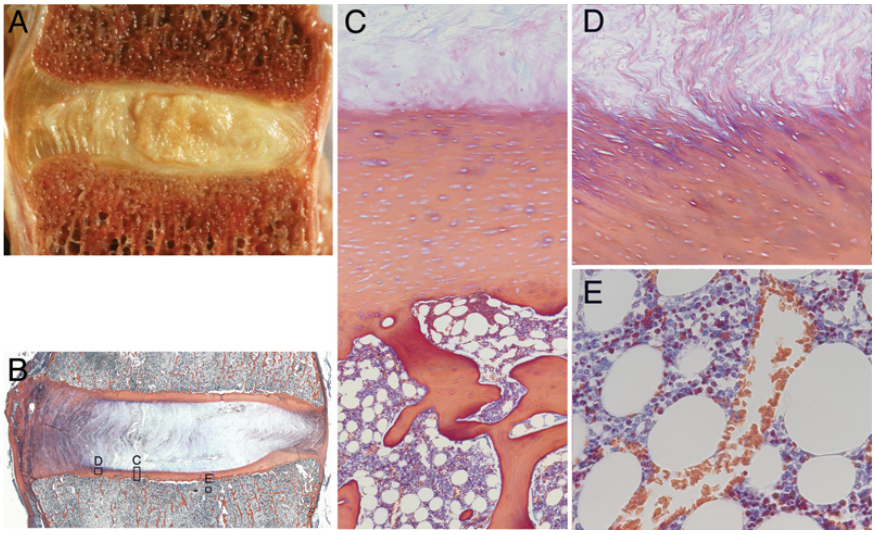

Figure 2.2: "(A) Gross morphology of the lumbar intervertebral joint. (B) Histology section showing regions of interest for panels C, D, and E. (C) End plate detail showing cartilaginous and bony components with hematopoietic marrow elements. (D) Insertion of annular fibers into the end plate cartilage at the inner annulus junction. (E) Vascular sinusoids in the marrow space adjacent to the end plate. Note for panels A and B, left side is anterior". Taken from Lotz *et al.* [15].

2.3. VERTEBRAE

The human spine consists of thirty-three vertebrae. In adults, the most caudal nine are fused into the sacrum and the coccyx [16]. The other twenty-four are categorised into three sections. The lower, or *lumbar*, back consists of the five largest vertebrae, conveniently named L1 to L5, and are situated between the rib cage and the pelvis. Figure 2.3(a) illustrates the outer anatomy of a lumbar vertebra whereas Figure 2.3(b) shows the internal bone structure of the *trabecular*. Like most bones, the vertebrae are made up of two types of bone. An outer dense *cortical* layer encapsulates the internal bone structure of the *trabecular* core which is made up of bony pillars, trabeculae, and voids. The vertebral body is connected to adjacent intervertebral discs through the end plates. A study by Zhao *et al.* [17] reports average L4 body height to be 30.1 mm. An observed average disc height of 11.3 mm results in a disc to vertebral body height ratio of approxi-

mately 2.7. The protrusions, or pedicles, are connected through ligaments and articular joints and prevent extreme movements of the vertebrae. Precise insights on load sharing between trabecular and cortical bone remains unclear. Even though trabecular bone accounts for most of the vertebral volume, Rockoff *et al.* [18] found cortical bone to be responsible for 45–75% of the vertebral peak strength. Eswaran *et al.* [19] found that this responsibility ranges from approximately 45% at the midtransverse section of the vertebral body to 15% near the end plates. Edwards *et al.* [13] reported a mean thickness of lumbar vertebral cortical bone to be 0.68 mm and not to correlate with age or gender.

The structural composition of bone is the result of a trade-off between rigidity and mass. Bone should be strong enough to withstand loads and forces and at the same time use a minimal volume. According to *Wolff's law*, bone structure adapts to mechanical stimuli or the lack of it [20]. Frost [21] provided the basis for the current *mechanostat* theory of bone adaptation by suggesting "that the most likely loading-derived stimulus for bone cells would be the strains developed in the bone tissue as a result of loading" [22]. Meakin *et al.* [22] summarises this theory as a negative feedback loop where (the absence of) mechanical strain causes bone mass and architecture to adapt accordingly. Bone mass and architecture remain unchanged under an optimal range of strain, *the lazy zone*, with 1250 ± 250 μstrain as target. In case of strains higher than this target range, bone formation takes places. Bone stiffness increases causing the strains to decrease. Alternatively, a strain magnitude below the lazy zone results in bone resorption. A decrease in stiffness follows to ensure re-establish optimal strain.

In a study on age-related changes in vertebral trabecular structure, Atkinson [23] gives various insights in bone resorption and formation and describes a difference in adaptation between horizontally and vertically oriented trabeculae. Internal demand for minerals causes lifelong ongoing bone resorption, a process that mostly affects trabecular bone. As stated earlier, bone forms in response to mechanical strains. Horizontally oriented trabeculae are hardly involved in direct weight-bearing and are therefore not imposed by high mechanical strains. These trabeculae diminish with age, which is in line with the fact that bone is continuously resorbed [24]. The same also goes for vertically oriented trabeculae, however, they stiffen at the same time as a result from larger mechanical strains. FE simulation of bone adaptation is further explained in Chapter 4, Section 4.1.

2.4. DISCUSSION

Literature was consulted to gain insight in the human lumbar anatomy. More specifically, the main components of a spinal unit - the intervertebral disc and the vertebrae - and the process of bone adaptation were studied. It was found that the intervertebral disc consists of two main components: the NP and the AF which, in turn, consists of ground matrix and collagen fibre bundles. The disc is connected to adjacent vertebrae through end plates that are bilayers of bone and cartilage (BEPS and CEPS, respectively). The vertebrae are made up of a spongy core that is encapsulated by a layer of cortical bone. The various components and corresponding properties must be taken into

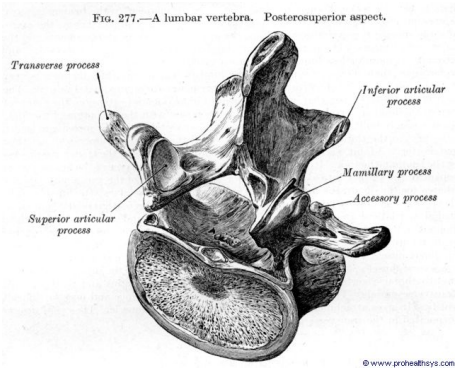

(a) "A lumbar vertebra from above and behind". Adapted from Gray and Lewis [25], retrieved from [26].

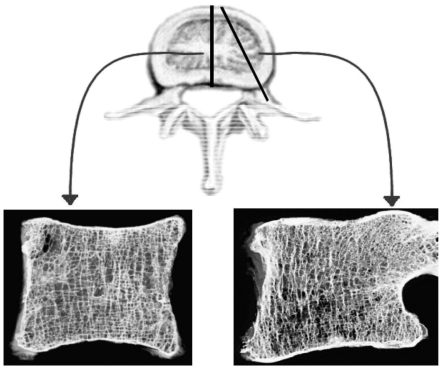

(b) "(Upper) 2 mm-thick slices of each vertebral body were obtained in the midsagittal plane, and in a para-sagittal plane passing through the pedicle. (Lower) A microradiograph of each slice was scanned at 400 DPI to produce greyscale images". Adapted from Zhao *et al.* [17].

Figure 2.3: Illustrations of the lumbar vertebrae.

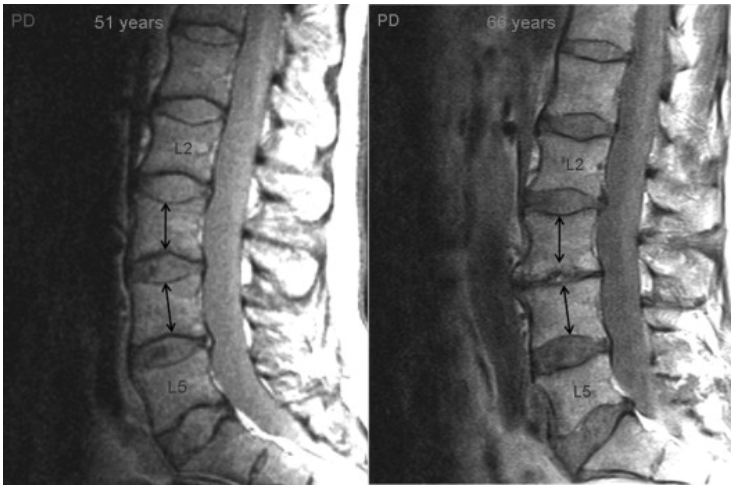

Figure 2.4: MR images of a 15-year follow-up study on ageing changes in the spine. A collapse of the L3–L4 and height increase in the adjacent vertebrae heights can be observed. Adapted from Videman *et al.* [27].

consideration when creating a model with the purpose of examining biomechanical behaviour of a spinal unit. Problems have arisen in studies on the NP, due to limitations in the ability to conduct *in vivo* experiments. Additionally, there is a lack of quantitative data on end plate characteristics. Approximations were used to create a model of a spinal unit as a means to answer this project's research question of understanding the biomechanical influence of the intervertebral disc on the adjacent vertebrae. The next chapter is a description on the process of creating an FE model.

REFERENCES

[1] M. A. Adams and P. J. Roughley, *What is intervertebral disc degeneration, and what causes it?* Spine **31**, 2151 (2006).

[2] N. Newell, J. Little, A. Christou, M. Adams, C. Adam, and S. Masouros, *Biomechanics of the human intervertebral disc: A review of testing techniques and results,* Journal of the mechanical behavior of biomedical materials **69**, 420 (2017).

[3] S. J. Ferguson and T. Steffen, *Biomechanics of the aging spine,* European Spine Journal **12**, S97 (2003).

[4] M. A. Adams and P. Dolan, *Intervertebral disc degeneration: evidence for two distinct phenotypes,* Journal of anatomy **221**, 497 (2012).

[5] K. M. Cheung, J. Karppinen, D. Chan, D. W. Ho, Y.-Q. Song, P. Sham, K. S. Cheah, J. C. Leong, and K. D. Luk, *Prevalence and pattern of lumbar magnetic resonance imaging changes in a population study of one thousand forty-three individuals,* Spine **34**, 934 (2009).

[6] E. I. de Schepper, J. Damen, J. B. van Meurs, A. Z. Ginai, M. Popham, A. Hofman, B. W. Koes, and S. M. Bierma-Zeinstra, *The association between lumbar disc degeneration and low back pain: the influence of age, gender, and individual radiographic features,* Spine **35**, 531 (2010).

[7] M. Adams, D. McMillan, T. Green, and P. Dolan, *Sustained loading generates stress concentrations in lumbar intervertebral discs,* Spine **21**, 434 (1996).

[8] S. Ebara, J. C. Iatridis, L. A. Setton, R. J. Foster, V. C. Mow, and M. Weidenbaum, *Tensile properties of nondegenerate human lumbar anulus fibrosus,* Spine **21**, 452 (1996).

[9] K. L. Markolf and J. M. Morris, *The structural components of the intervertebral disc: a study of their contributions to the ability of the disc to withstand compressive forces,* JBJS **56**, 675 (1974).

[10] D. A. Neumann, *Kinesiology of the Musculoskeletal System-E-Book: Foundations for Rehabilitation* (Elsevier Health Sciences, 2013).

[11] N. Bogduk, *Clinical and Radiological Anatomy of the Lumbar Spine E-Book* (Elsevier Health Sciences, 2012).

[12] R. J. Moore, *The vertebral end-plate: what do we know?* European Spine Journal **9**, 92 (2000).

[13] W. T. Edwards, Y. Zheng, L. A. Ferrara, and H. A. Yuan, *Structural features and thickness of the vertebral cortex in the thoracolumbar spine,* Spine **26**, 218 (2001).

[14] S. Roberts, I. McCall, J. Menage, M. Haddaway, and S. Eisenstein, *Does the thickness of the vertebral subchondral bone reflect the composition of the intervertebral disc?* European Spine Journal **6**, 385 (1997).

[15] J. Lotz, A. Fields, and E. Liebenberg, *The role of the vertebral end plate in low back pain,* Global spine journal **3**, 153 (2013).

[16] R. Drake, A. W. Vogl, and A. W. Mitchell, *Gray's Anatomy for Students International Edition: With STUDENT CONSULT Online Access* (Elsevier Health Sciences, 2009).

[17] F.-D. Zhao, P. Pollintine, B. Hole, M. Adams, and P. Dolan, *Vertebral fractures usually affect the cranial endplate because it is thinner and supported by less-dense trabecular bone,* Bone **44**, 372 (2009).

[18] S. D. Rockoff, E. Sweet, and J. Bleustein, *The relative contribution of trabecular and cortical bone to the strength of human lumbar vertebrae,* Calcified Tissue Research **3**, 163 (1969).

[19] S. K. Eswaran, A. Gupta, M. F. Adams, and T. M. Keaveny, *Cortical and trabecular load sharing in the human vertebral body,* Journal of Bone and Mineral Research **21**, 307 (2006).

[20] J. Wolff, *The law of bone remodelling* (Springer Science & Business Media, 2012).

[21] H. M. Frost, *The utah paradigm of skeletal physiology: an overview of its insights for bone, cartilage and collagenous tissue organs,* Journal of bone and mineral metabolism **18**, 305 (2000).

[22] L. B. Meakin, J. S. Price, and L. E. Lanyon, *The contribution of experimental in vivo models to understanding the mechanisms of adaptation to mechanical loading in bone,* Frontiers in endocrinology **5**, 154 (2014).

[23] P. Atkinson, *Variation in trabecular structure of vertebrae with age,* Calcified tissue research **1**, 24 (1967).

[24] L. Mosekilde, *Age-related changes in vertebral trabecular bone architecture—assessed by a new method,* Bone **9**, 247 (1988).

[25] H. Gray and W. Lewis, *Anatomy of the human body. 20th,* Philadelphia and New York, Lea & Febiger (1918).

[26] *Prohealthsys: Vertebral column,* https://prohealthsys.com/central/anatomy/grays-anatomy/index-10/index-10-2-2/lumbar_vertebra/, accessed: 2019-02-16.

[27] T. Videman, M. C. Battié, L. E. Gibbons, and K. Gill, *Aging changes in lumbar discs and vertebrae and their interaction: a 15-year follow-up study,* The Spine Journal **14**, 469 (2014).

3

FINITE ELEMENT MODEL

The goal of this project is to gain insight in the influence of an intervertebral disc on its adjacent vertebrae. As mentioned in first chapter, the FEM can be used to assess biomechanics [1]. Section 3.1 describes the general working method of the FEM, after which a detailed explanation of this project's modelling and validation processes follow..

3.1. INTRODUCTION TO THE FINITE ELEMENT METHOD

The finite element method (FEM) is a means of assessing a large problem by breaking it down into a number of smaller and simpler sub-problems by performing a finite element analysis (FEA). The principle of FEA is particularly useful in engineering for calculations of stresses and strains. A body is partitioned by meshing it into a finite number of elements and partial differential equations are solved for those separate elements. These separate solutions can be combined into matrix-form and consequently computer solved, making the FEM a very efficient manner of assessing complex geometries. This is especially useful in biomechanics, as biological tissues hardly ever have a simple geometry. Choosing an appropriate meshing method is necessary for efficiently acquiring reliable and accurate data. Partitioning is further elaborated in the following sections.

3.1.1. CONTINUUM MODELLING APPROACH

A common way of using the FEM is to partition a body into a finite number of *continuum* elements, meaning that the entire body is assessed as one solid *continuum* with every element getting assigned specific material properties. However, not all biological tissues are continuous. As explained in previous chapter, trabecular bone is a porous structure comprising of trabecular pillars and voids. Nevertheless, Phillips *et al.* [2] state that it is quite common to use a continuum mechanics approach for modelling bone and they explain that there are three ways of dealing with the issue mentioned before.

The two generally accepted methods that Phillips *et al.* [2] describe, are called *microscale* and *macroscale* continuum modelling. The first requires the size of one finite element to

be smaller than or corresponding to one structural element of bone. In the continuum part, all elements are considered either 'bone' or 'not bone'. Specific material properties are assigned to the 'bone' elements and the 'not bone' elements can be modelled as voids. The second - macroscale - approach deems the entire structure as one continuum and consequently, voids are not modelled. Empirically established material properties are assigned to the elements, to make the entire structure behave as bone. Both of these approaches are the result of a trade-off between accuracy and computational efficiency. The *microscale* approach often uses μMRI or μCT data to create a highly accurate model of bone structure whereas the *macroscale* approach is more of an approximate calculation, heavily relying on empirical data. Due to the large number of elements, the *microscale* approach is computationally demanding whereas the *macroscale* approach performs calculations more efficiently.

To overcome this trade-off, a *mesoscale* alternative was recommended. Rather than only continuum elements, various structural elements can be used to represent the structural nature of bone [2]. As an example, [2] write that truss and shell elements can serve as trabecular and cortical bone, respectively. This structural *mesoscale* approach enables the FE model to perform with fewer elements and simultaneously ensures the elements to behave more accordingly to the structure they represent. It is considered to reach both *microscale* accuracy as well as *macroscale* computational efficiency. Because of the variety of materials and elements in the spinal elements (elaborated on in the previous Chapter), a hybrid *mesoscale* approach was selected for creating this project. This approach will ensure the FEA results to be more accurate and computationally efficient than either a *micro-* or *macroscale* modelling method. Elaboration on the modelling approach for this project is described in Section 3.3.

3.1.2. FINITE ELEMENT MODELS OF INTERVERTEBRAL DISCS

A systematic review was conducted to investigate previously developed FE models of human intervertebral discs. Nine models were found and assessed on various factors [3–11]. Modelling approach, element types and material properties were of most interest. All models used a continuum approach for the AF ground matrix. The AF fibres were often structurally modelled as truss, cable or spring elements [3–5, 7, 8, 11], but also as parametrically determined material properties within the AF [6, 10]. Like the AF, the NP was modelled as solid continuum elements. Although Chosa *et al.* [3] did not report the specific use of elements, they mention using direct input of intradiscal pressure that they derived from literature. This resembles the approach by Newell *et al.* [12], who have modelled the NP as a pressurised cavity.

After establishing a working geometrical model of a spinal unit, the model must be validated for appropriate material properties. However, validation of intervertebral disc FE models has proven to be difficult. Proper *in vivo* data are essentially impossible to obtain without invasive methods. *In vitro* experiments are ideally performed on freshly harvested discs but in practice, they have generally been deep frozen. Literature is disagreeing about the influence of deep freezing on disc biomechanics [13]. Section 3.5 elaborates on the validation method for this project.

3.2. MATERIALS

The main software used for this project are Abaqus/CAE version 6.13 [14] and MATLAB version R2014a [15]. The first is a software suite under the SIMULIA platform by Dassault Systèmes. Besides being an analogy to 'Computer Aided Engineering', 'CAE' stands for 'Complete Abaqus Environment', meaning it provides an evironment for the modelling process as well as FEA and visualisation of the FEA. The second is a numerical computing software that can be used for matrix calculations and scripting of algorithms.

3.3. METHOD: BUILDING A MESH

To build an FE model for analysis, there are multiple factors to take into consideration. Besides the appropriate choice of element types and material properties, mesh generation also has an influence on analysis outcomes and success rates [16]. Abaqus/CAE was used for automated mesh generation of the spinal unit and the building process of the resulting model is set forth in the following subsections.

3.3.1. MODEL I: ABAQUS GEOMETRY

Abaqus/CAE was used to create a cylinder with the approximate dimensions of a spinal unit (vertebra-disc-vertebra) and two steel components on either end of the cylinder for compressional simulations. It should be noted that the disc and vertebral body are kidney-shaped. To increase computational efficiency by reducing the amount of variables however, it was decided to create a simple geometry and therefore the cylinder has a circular base. Figure 3.1 shows a visualisation of this first model. The cylinder was sectioned according to average heights of the spinal parts and the disc was sectioned to have a core and surrounding layer acting as NP and AF, respectively. For the mesh controls, it was decided to use *hex* (hexahedral) shaped solid elements (type C3D8H) and a default *sweep* technique that follows an algorithm based on the *medial axis* of the unit. Section 17.7.6 from the Abaqus 6.14 User's Guide [17] explains that "Abaqus/CAE generates hexahedral and hexahedral-dominated meshes by sweeping the quadrilateral and quadrilateral-dominated elements generated by the two algorithms from the source side to the target side". The Guide further notes that for a simple geometry with a large number of elements, this Medial axis algorithm is a computationally more efficient option than the Advancing front algorithm. Considering a cylinder to be a relatively simple geometry, this Medial axis algorithm was chosen, after which 80 seeds were evenly spread over cylinder's circumference. Meshing the unit resulted in an AF consisting of five vertically stacked layers.

ADDITION OF MATLAB TRUSSES

To simulate the presence of collagen fibres in the AF, it was decided to add truss T3D2 elements to the AF section. However, as Abaqus did not allow this type of feature, the input file of the meshed cylinder was exported and manually adjusted using MATLAB. A script was configured to rewrite the input file so that truss elements were created between AF nodes in a fashion that diagonally orientated fibres would be formed, alternating per layer of the AF (see Figure 3.1(c)). Basic boundary and loading conditions were created within Abaqus by constraining the lower steel plate from movement and rotation in all

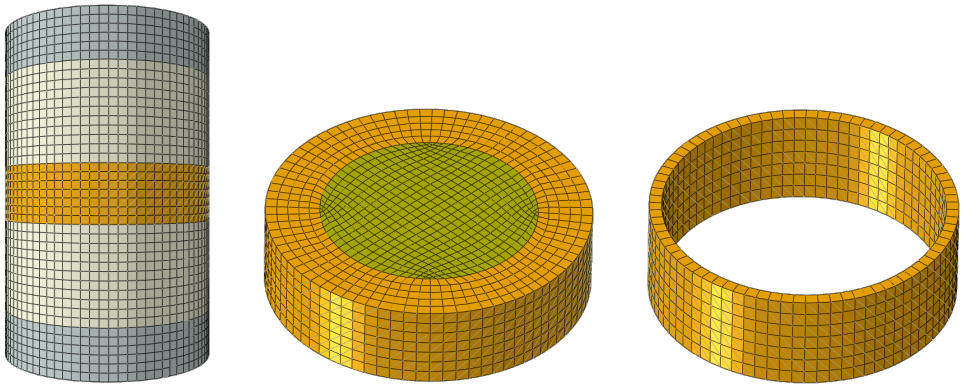

(a) Complete unit with steel plates (grey), vertebrae (white) and AF (orange).

(b) Disc with NP (yellow), AF ground matrix (orange) and fibres (grey).

(c) Outer lamella with alternating fibre orientation.

Figure 3.1: Visualisation of the first model made in Abaqus.
Colour legend: Gray: steel components, Orange: AF, Yellow: NP and White: vertebrae.

directions and applying a load of 100N on the top steel plate. After submitting the model for analysis, Abaqus returned a warning displaying that several elements were distorted. These elements were identified and displayed in red in Figures 3.2(a) and 3.2(b).

ALTERNATIVE MESHING METHOD

It seemed that the cylindrical shape posed a problem for the default meshing technique that was selected in Abaqus. This was confirmed by a review from Lan and Lo [18] who studied several methods and wrote that curved surfaces in particular are difficult to discretise and the more common methods often causes element distortion. This warning was reason for applying other Abaqus meshing methods. Different element shapes were tested and eventually an approach using a *sweep* technique based on an *Advancing front* algorithm was tested. The Abaqus 6.14 User's Guide explain this method as follows: "[t]he advancing front algorithm generates quadrilateral elements at the boundary of the region and continues to generate quadrilateral elements as it moves systematically to the interior of the region" [17]. The new mesh (Figure 3.2(c)) did not cause element distortion but it was feared that the random organisation of elements would give less reproducible FEA results than a more structured one. Therefore, it was decided not to create a model within the Abaqus/CAE environment but only to use the program for the actual FEA.

3.3.2. MODEL II: MATLAB GEOMETRY

The approach of sketching the model's geometry in Abaqus was discarded and the entire model was created by writing a novel input file in MATLAB. A study on mesh generation methods by Ho-Le [16] was consulted after which the node generation approach was adopted to develop a 2D model of the disc (Figure 3.3(a)). The squares and surround-

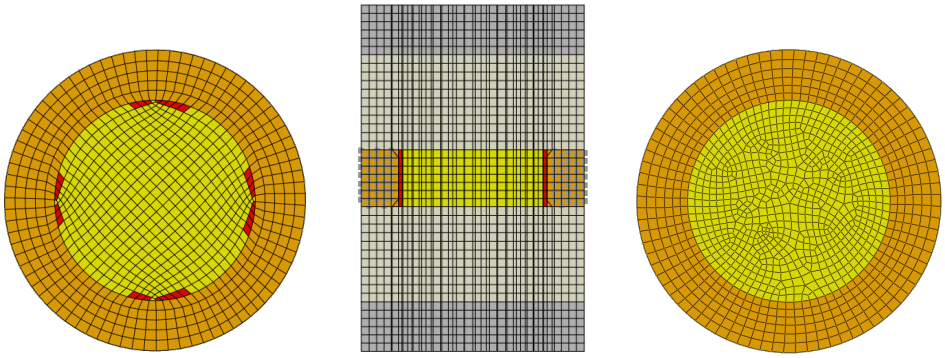

(a) Top view of intervertebral disc. Meshing algorithm: Medial axis.

(b) Median sagittal view of the entire spinal unit. Meshing algorithm: Medial axis.

(c) Top view of intervertebral disc. Meshing algorithm: Advancing front.

Figure 3.2: Visualisation of the two meshing methods in `Abaqus`.
Yellow: NP, orange: AF with grey AF fibres, White: bone, grey: steel, red: distortion after analysis

ing quadrilaterals that represent the NP become hexahedral elements after conversion to a three dimensional model. An elliptical rather than circular shape was considered but eventually rejected due the risk of decreasing homogeneity of the element size and shape and subsequently, FEA accuracy. The variable parameters that are the base of the two dimensional mesh were the unit diameter (mm), NP diameter (mm), number of circumferential seeds and the number of lamellae. This two dimensional base was used to create a three dimensional model by copying the two dimensional layer of nodes on a third axis. The result of this transformation can be observed in Figure 3.3. The model's requirements and former parameters and default input values were revised. The definite set of parameters and values that were used for establishing the model can be found in Table 3.1.

A difference between the initial set of parameters and the adopted set is the change from one unit diameter to two. As stated earlier, the human intervertebral disc is kidney-shaped rather than round. Instead of one diameter (for a circular shape), experimental data from Newell *et al.* [12] reported two average diameters for the investigated discs. These two diameters were used to calculate the average surface and this in turn, was used to calculate one average diameter for a circle-shaped disc model. The AF is usually made up of 15 to 25 lamellae [13], but due to the trade-off between a coarse/efficient and detailed/slow processing model it was chosen to reduce that number. The chosen values for the number of vertical layers and seeds was a result of this. The ratio representing the NP box to diameter ratio is to create an offset between the 'box' and true NP circumference. The reason for this is to ensure the corner elements in the NP remain hexahedral and will not cause distortion. This offset is clearly visible in Figure 3.4(c), as opposed to the initial geometry without offset (Figure 3.3(a)). Besides the geometrical parameters, material properties and loading and boundary conditions can also be adjusted in the

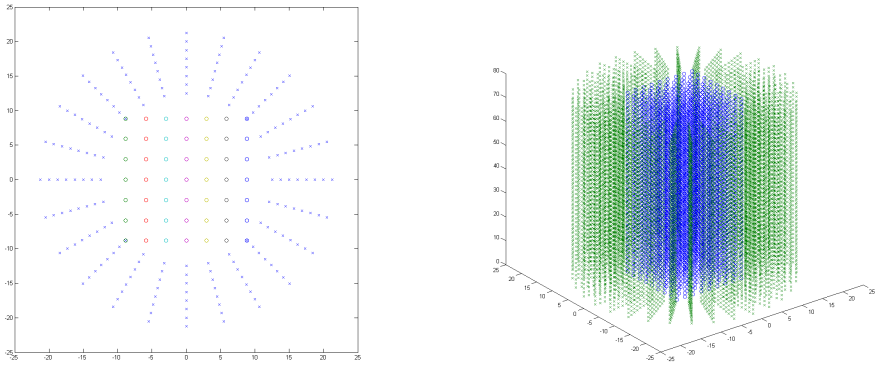

(a) 2D structure (b) 3D structure

Figure 3.3: MATLAB plots of node distribution for FE mesh.

MATLAB script.

Further steps were taken towards creating a complete model with all required elements. The base of the model is a solid continuum but structural elements were added to simulate collagen fibres, cortical bone and end plates. The first step was to write a parametric script that would create truss elements between the diagonal nodes of the hexahedral AF elements. The number of collagen 'fibres' in the model would consequently be defined by the number of AF vertical layers and lamellae. As this number would not nearly approximate the true number of collagen bundles in the human disc, a ratio of 17.8 % (volume of fibres relative to the volume of AF ground matrix) was used to calculate the thickness of the truss elements [12]. The cortical bone and end plates were modelled with the use of 5-point integration shell elements. The shells for the axial cortical bone, BEPS and CEPS were derived from the outer nodes of the vertebral and disc continuum elements, respectively. The thickness for cortical bone derived from literature but, as explained in Section 2.2 of the previous Chapter, there is a lack of quantitative data on the end plates. Values on thickness of end plates were found but no distinction was made between the bony or cartilaginous part of the plates. It was observed, however, that the BEPS were generally thinner than the CEPS and therefore, a parametric ratio of 0.3 (BEPS) to 0.7 (CEPS) was set. It should be noted that during material sensitivity tests (Section 3.5.1), it was found that this ratio was had hardly any influence on the results of the FEA. Also, the script was adjusted to simplify sectioning. Following this enhancement, the model could effectively be extended or halved which was useful for i.e. analyses on the disc (model: one disc and two half vertebrae) and on the vertebra (model: two half vertebrae, two discs, and one whole vertebra).

3.4. RESULTS: FINAL GEOMETRY

The final model of part of the lumbar spine was created by writing an input file in MATLAB to render and perform finite element analyses on in Abaqus/CAE. The rendered model is visualised in Figure 3.4. The choices of element and various adjustable parameters can be found in tables 3.2 and 3.1, respectively. Appropriate material properties from literature were assigned to the various sections to ensure the model runs without producing errors.

Parameter	Value
Unit diameters (mm)	54, 40*
Disc height (mm)	10.08*
Disc to vertebra height ratio	2.7**
Number of vertical layers in one disc	6
Number of lamellae	9
Number of circumferential seeds	32
NP box to diameter ratio	0.9
NP to AF surface ratio	0.29*
Fibre to AF volume ratio	0.178*
Fibre angle to horizontal	28 °***
Bony to cartilage end plate ratio	0.3

Table 3.1: Parameters and chosen input values for MATLAB mesh.
*Values were obtained from experimental data by Newell *et al.* [12].
** Values for the calculation of this ratio were derived from Zhao *et al.* [19].
*** Angle was calculated as the diagonal of one outer anulus element disc height & number of vertical disc layers.

Tissue	Element type	Abaqus element
Trabecular bone	Solid hexahedral	C3D8H
Cortical bone	Solid shell	S4
CEPS	Solid shell	S4
BEPS	Solid shell	S4
AF Fibres	Truss	T3D2
AF Ground Matrix	Solid hexahedral	C3D8H
NP	Solid hexahedral	C3D8H

Table 3.2: Element types for all sections

3.5. VALIDATION

To determine appropriate material properties, a material sensitivity study can be performed. Details on the study are described in Subsection 3.5.1 below. Subsection 3.6 then elaborates on how this test was used to validate the FE model.

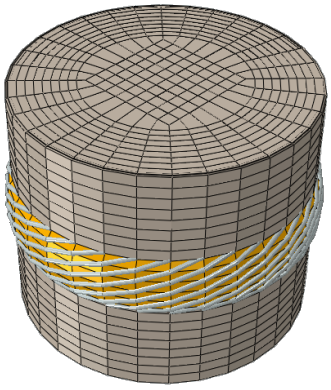

(a) Full view of a spinal unit after deformation.

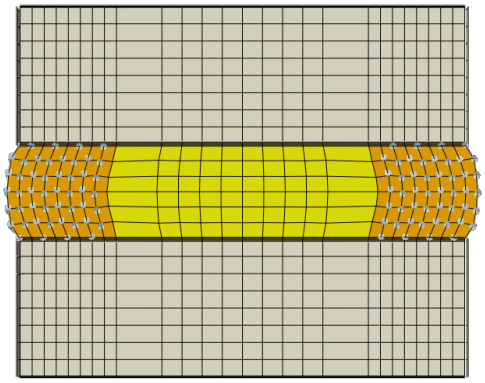

(b) Sagittal view of a spinal unit after deformation.

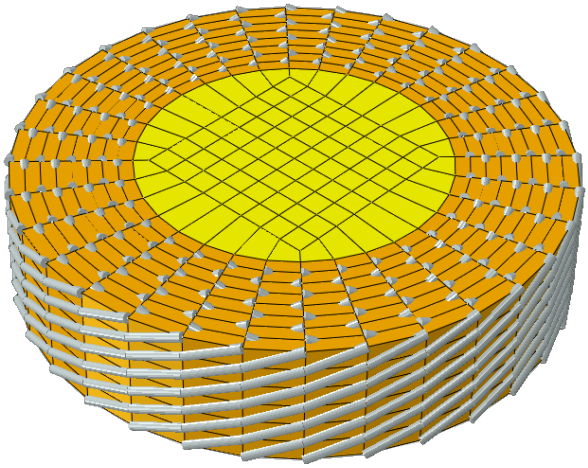

(c) The intervertebral disc with all components.

Figure 3.4: Rendered view of the FE model of one spinal unit.
Yellow: NP, orange: AF ground matrix, White: bone, grey: AF fibres, beige: cortical bone and end plates.

3.5.1. MATERIAL SENSITIVITY STUDY

Appropriate values for the model's material property parameters had to be assigned. It was found in literature that there is a large variety in material properties of FE models of human lumbar intervertebral discs. Studies by Xie *et al.* [11] compared elastic to hyperelastic properties for the intervertebral disc and found that the latter described the disc behaviour more accurately. Hyperelastic behaviour can be expressed in various models, of which the Neo-Hookean approach is a relatively simple and efficient option. It describes stress-strain behaviour of hyperelastic materials in terms of two unitless constants, C_1 and D, respectively. C_1 is a material constant based on an invariant (I_1) of the Cauchy-Green tensor (C_1) that describes deformation in terms of local change in distances within a material. $D = 0$ for incompressible Neo-Hookean materials [20]. The function of a Neo-Hookean material (W) is described according to Equation 3.1. Both Xie *et al.* [11] and Newell *et al.* [12] have adopted a Neo-Hookean model to describe the non-linear hyperelastic and incompressible behaviour of the AF ground substance.

$$W = C_1(I_1 - 3) \tag{3.1}$$

Suitable material properties were defined by performing a two-step material sensitivity study. The first study was meant to find which of the disc's components (the NP, AF ground substance or the collagen fibres) had the biggest influence on the disc's behaviour under compressional loading. Initial properties from a similar model by Newell *et al.* [12] were used. However, the NP was modelled as a pressurised cavity rather than continuum elements. The approach by Adam *et al.* [21] was therefore used for the NP values, who assigned NP properties of an 'order of magnitude less stiff than the AF ground substance while maintaining near-incompressible material behaviour'. For the material sensitivity test, this approach was deployed by setting the initial NP's C_1 according to Equation 3.2 and adjusting it accordingly throughout the test.

$$C_{1,\mathrm{NP}} = 0.1 \cdot C_{1,\mathrm{AF}} \tag{3.2}$$

This first assessment of material properties showed that altering the AF properties resulted in the biggest changes in behaviour, whereas changes in NP did not. The ground substance (the continuum elements representing the AF) influenced the disc's absolute stiffness, whereas the trusses that represent the fibre bundles had an impact on the exponential shape of the curve that corresponds to hyperelasticity. Initial bone material properties are expected to change after running the bone adaptation algorithm, therefore the value that was of most interest was the chosen ratio of BEPS thickness relative to the CEPS thickness. Changing this ratio, however, did not have significant influence and it was therefore kept at the initial value. Based on these findings, a second sensitivity study was conducted to define the appropriate values for the AF components.

Pressure simulations were performed and results were compared to an experimental study by Newell *et al.* [12]. This study analysed geometry and compressional behaviour of 16 healthy lumbar intervertebral discs. The average geometry reported in this study

was used for the FE model and the average force-displacement curve of all tests on all discs was used as a reference for the material sensitivity test. The average displacement of the results is represented by the black curve named *Experimental Data (Newell, 2019)* in Figure 3.5. After finding the AF ground matrix and collagen fibres to be most influential to the disc's behaviour, these were varied in order for the model's output to approach experimental data from Newell *et al.* [12]. The results of this compressibility analysis can be observed in Figure 3.5. To see how the FE model's compressional behaviour (red curve) compares to the experimental study by Newell *et al.* [12], see Figure 3.6. The most fitting material properties were consequently used for further analyses. They are summarised in Table 3.3.

3.5.2. VALIDATION

Validation of the FE model is necessary to ensure accurate and reliable results from the FEA. In other words, it must be confirmed that the model will produce realistic results. As explained earlier in this chapter, validation of intervertebral discs has proved difficult due to limitations in *in vivo* experimenting. The second part of the material sensitivity test described in the previous section was performed by comparing experimental data from a study that performed compression tests on intervertebral discs to results of a simulation of that study on the FE model. By choosing the definitive material properties that ensure the model to produce results similar to experimental data, the model was effectively validated.

Tissue	**Young's Modulus (MPa)**	**Poisson's ratio**	**Thickness (mm)**	**Reference**
Trabecular bone	10,400	0.3		[22, 23]
Cortical bone	18,600	0.3		[22, 23]
CEPS	23.8	0.4	0.406	[24]
BEPS	18,600	0.3	0.174	[22, 23]
AF Fibres	306.16	0.35		
Neo-Hookean material	$\mathbf{C_1}$	**D**		
AF Ground Matrix	0.0218	0		
NP	0.00218	0		

Table 3.3: Material properties deployed after material sensitivity study

3.6. DISCUSSION

A semi-continuum approach of the FEM was adopted to create a model of a spinal unit (one disc, two vertebrae, two BEPS and two CEPS). With the purpose of increasing computational efficiency, it was decided to create a purely cylindrical model without ligaments and vertebral pedicles. The disc consists of two continuum sections, functioning as the NP and AF, and structural truss elements acting as the collagen fibres. The trabecular part of a vertebral body is modelled in continuum elements whereas the cortical bone and end plates are approached by structural shell elements. After failed attempts to create a robust model in `Abaqus/CAE`, a `MATLAB` script was written to create an input file to

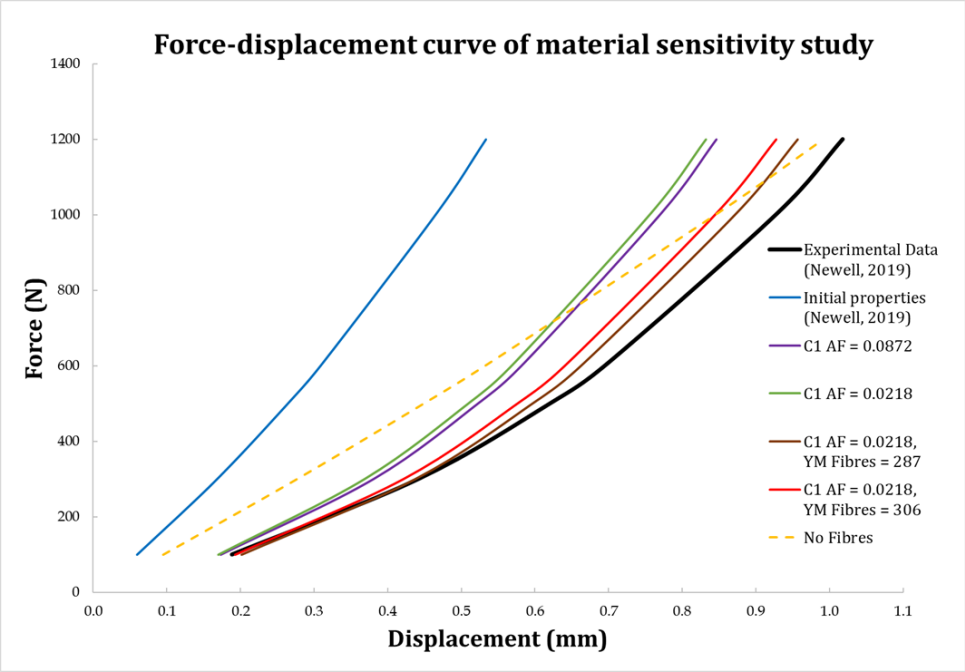

Figure 3.5: Graphical results of the sensitivity study on FEA material properties. C1 indicates the first material coefficient of the Neo-Hookean model and FYM stands for the Young's Modulus (MPa) of the AF collagen fibres.

be used in `Abaqus/CAE` for FEA.

Prior to performing valuable analyses, accurate material properties have to be determined. This was achieved by performing a two-fold material sensitivity study. After first investigating which material properties were most influential for model behaviour, experimental data on human lumbar intervertebral discs were used to approach the most fitting values for these material properties. The definitive properties generated model behaviour that was considered comparable to the results of that study. As a consequence, this material sensitivity study also served as a means to validate the model. However, it should be noted that only *in vitro* uniaxial compression tests were used for this study. Hence, the model has only been validated for one type of loading. The following chapter will cover an extensive outline of the analyses that simulate bone adaptation in the vertebrae.

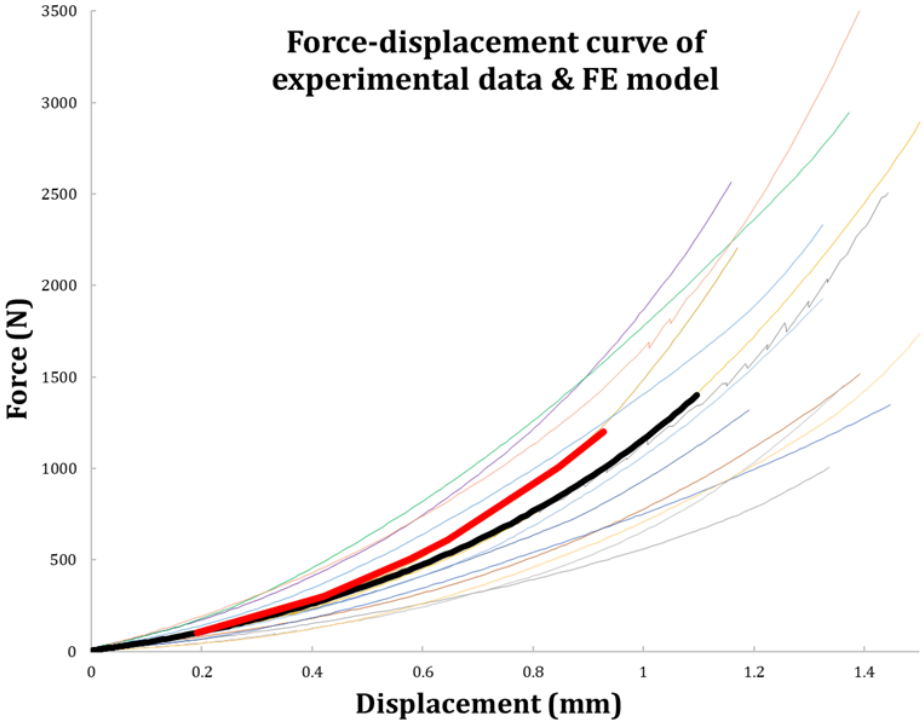

Figure 3.6: Comparison of FE model force-displacement to experimental data from Newell *et al.* [12]. The black curve represents the average curve for all experiments (the sixteen thin curves). The red curve corresponds to the FE model with definitive material properties

REFERENCES

[1] H. Schmidt, F. Galbusera, A. Rohlmann, and A. Shirazi-Adl, *What have we learned from finite element model studies of lumbar intervertebral discs in the past four decades?* Journal of biomechanics **46**, 2342 (2013).

[2] A. T. Phillips, C. C. Villette, and L. Modenese, *Femoral bone mesoscale structural architecture prediction using musculoskeletal and finite element modelling,* International Biomechanics **2**, 43 (2015).

[3] E. Chosa, K. Goto, K. Totoribe, and N. Tajima, *Analysis of the effect of lumbar spine fusion on the superior adjacent intervertebral disk in the presence of disk degeneration, using the three-dimensional finite element method,* Clinical Spine Surgery **17**, 134 (2004).

[4] M. Fagan, S. Julian, D. Siddall, and A. Mohsen, *Patient-specific spine models. part 1: Finite element analysis of the lumbar intervertebral disc—a material sensitivity study,* Proceedings of the Institution of Mechanical Engineers, Part H: Journal of Engineering in Medicine **216**, 299 (2002).

[5] F. S. Gómez, R. L. Lorza, M. C. Bobadilla, and R. E. García, *Improving the process of adjusting the parameters of finite element models of healthy human intervertebral discs by the multi-response surface method,* Materials **10**, 1116 (2017).

[6] N. T. Jacobs, D. H. Cortes, J. M. Peloquin, E. J. Vresilovic, and D. M. Elliott, *Validation and application of an intervertebral disc finite element model utilizing independently constructed tissue-level constitutive formulations that are nonlinear, anisotropic, and time-dependent,* Journal of biomechanics **47**, 2540 (2014).

[7] C.-K. Lee, Y. E. Kim, C.-S. Lee, Y.-M. Hong, J.-M. Jung, and V. K. Goel, *Impact response of the intervertebral disc in a finite-element model,* Spine **25**, 2431 (2000).

[8] M. Masni-Azian & Tanaka, *Statistical factorial analysis approach for parameter calibration on material nonlinearity of intervertebral disc finite element model,* Computer methods in biomechanics and biomedical engineering **20**, 1066 (2017).

[9] H. Schmidt, F. Galbusera, H.-J. Wilke, and A. Shirazi-Adl, *Remedy for fictive negative pressures in biphasic finite element models of the intervertebral disc during unloading,* Computer methods in biomechanics and biomedical engineering **14**, 293 (2011).

[10] Y. Schroeder, W. Wilson, J. M. Huyghe, and F. P. Baaijens, *Osmoviscoelastic finite element model of the intervertebral disc,* European spine journal **15**, 361 (2006).

[11] F. Xie, H. Zhou, W. Zhao, and L. Huang, *A comparative study on the mechanical behavior of intervertebral disc using hyperelastic finite element model,* Technology and Health Care **25**, 177 (2017).

[12] N. Newell, D. Carpanen, G. Girgoriadis, J. Little, and S. Masouros, *Material properties of degenerate and non-degenerate human lumbar intervertebral discs across strain rates,* JMBBM (Under Revision, 2019).

[13] N. Newell, J. Little, A. Christou, M. Adams, C. Adam, and S. Masouros, *Biomechanics of the human intervertebral disc: A review of testing techniques and results,* Journal of the mechanical behavior of biomedical materials **69**, 420 (2017).

[14] Hibbett, Karlsson, and Sorensen, *ABAQUS/standard: User's Manual*, Vol. 1 (Hibbitt, Karlsson & Sorensen, 1998).

[15] I. Mathworks, *Matlab: R2014a,* Mathworks Inc, Natick (2014).

[16] K. Ho-Le, *Finite element mesh generation methods: a review and classification,* Computer-aided design **20**, 27 (1988).

[17] D. Systèmes, *Abaqus analysis user's guide, version 6.14,* (2014).

[18] T. Lan and S. Lo, *Finite element mesh generation over analytical curved surfaces,* Computers & Structures **59**, 301 (1996).

[19] F.-D. Zhao, P. Pollintine, B. Hole, M. Adams, and P. Dolan, *Vertebral fractures usually affect the cranial endplate because it is thinner and supported by less-dense trabecular bone,* Bone **44**, 372 (2009).

[20] B. Kim, S. B. Lee, J. Lee, S. Cho, H. Park, S. Yeom, and S. H. Park, *A comparison among neo-hookean model, mooney-rivlin model, and ogden model for chloroprene rubber,* International Journal of Precision Engineering and Manufacturing **13**, 759 (2012).

[21] C. Adam, P. Rouch, and W. Skalli, *Inter-lamellar shear resistance confers compressive stiffness in the intervertebral disc: An image-based modelling study on the bovine caudal disc,* Journal of Biomechanics **48**, 4303 (2015).

[22] J. Y. Rho, R. B. Ashman, and C. H. Turner, *Young's modulus of trabecular and cortical bone material: ultrasonic and microtensile measurements,* Journal of biomechanics **26**, 111 (1993).

[23] T. M. Keaveny and W. C. Hayes, *A 20-year perspective on the mechanical properties of trabecular bone,* Journal of biomechanical engineering **115**, 534 (1993).

[24] H. Yamada, F. G. Evans, *et al.*, *Strength of biological materials,* (1970).

4

FINITE ELEMENT ANALYSIS

To answer this project's research question, an assessment of spinal biomechanics was performed with FEA. The building process of the FE base model was described in the previous chapter. This chapter will elaborate on the analyses that were run to give insight into the influence of the intervertebral disc on adjacent vertebrae.

4.1. BONE ADAPTATION IN FINITE ELEMENT ANALYSES

As explained in Section 2.3, bone adapts to mechanical influences. When FEM became an appropriate method to assess biomechanics, Turner [1] established "three fundamental rules that govern bone adaptation [from which] several mathematical equations can be derived that provide simple parametric models for bone adaptation". In 2014, Geraldes and Phillips [2] proposed a new optimisation algorithm for orthotropic bone adaptation in FE models. The algorithm operates by assigning initial material properties to all bone elements, running iterative FE analyses and extracting the internal maximal principal strains from those elements. These strains are then used to calculate and approach the true material properties that allow the bone to function under an optimal target strain, also defined as *the lazy zone*, of 1250 ± 250 μstrain [3]. The process continues until a certain proportion of elements reaches the *lazy zone*. Equation 4.1 shows the iterative calculation for a bone element's Young's Modulus (E_i^{it}) by multiplying the modulus of previous iteration with a coefficient calculated from the absolute maximum principal local strain (ε_{max}) that occurs in the element and the target strain (ε_{nt}) [4, 5].

$$E_i^{it} = E_i^{it-1} \frac{|\varepsilon_{max}^{it}|}{\varepsilon_{nt}} \tag{4.1}$$

4.2. MATERIALS

The main software used for this project are `Abaqus/CAE` version 6.13 [6] and `MATLAB` version R2014a [7]. The bone adaptation algorithm was written and operated in `MATLAB`

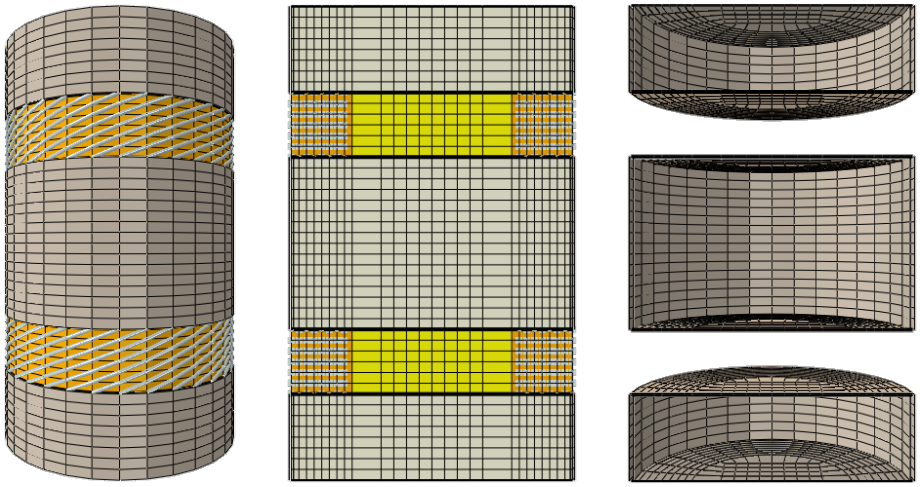

(a) Frontal view. (b) Median sagittal view. (c) Shell elements representing cortical bone and end plates

Figure 4.1: Rendered view of the FE model of two spinal units.
Yellow: NP, orange: AF ground matrix, White: bone, grey: AF fibres, beige: cortical bone and end plates.

while making use of the `Abaqus/CAE` environment for FEA and of `PYTHON`[8] to extract data from those analyses.

4.3. METHODS

For the material sensitivity study on the intervertebral disc, an FE model of one spinal unit (one disc, two halve vertebrae) was developed. Assessing biomechanics in a whole vertebrae, however, required doubling the model. This resulted in two spinal units (two discs, two halve vertebrae and one whole vertebra in the middle) which is visualised in Figure 4.1. After validation of the model, the bone adaptation algorithm had to be incorporated into the previously written `MATLAB` script for creating the input file. This process is discussed in Subsection 4.1.

The algorithm used for this project was derived from a study by Zaharie and Phillips [9]. This version of the algorithm was written to approach orthotropic bone adaptation. To enable orthotropy, material properties in the form of engineering constants were assigned to the bone elements. Both stresses and strains for all directions are extracted from the FEA to approach bone adaptation. To increase computational efficiency, and because only axial loading will be tested in this project, the algorithm was adjusted to simulate isotropic adaptation. Only absolute maximal principal strains were extracted, rather than normal strains for all directions and shear stresses. Material properties of bone are expressed in Young's Modulus and Poisson's ratio. The latter is often assumed to be 0.3 for bone in structural analyses and was therefore kept constant [10]. To ac-

count for trabecular bone adaptation, Equation 4.1 was used as a basis in the MATLAB script for adaptation. A similar approach was used to approach cortical bone adaptation. However, rather than changing the Young's Modulus, the thickness of cortical bone was iteratively adjusted. In this preliminary phase of the research, FE analyses were only performed with axial loading conditions and therefore it was decided to only take unidirectional strains into consideration.

The adaptation was first run on the FE model with material properties corresponding to a healthy intervertebral disc, as elaborated on in Section 3.5.1. For this simulation, initial material properties of bone were taken from literature [10, 11]. These properties can be found in Table 3.3. A uniformly spread total force of 500 N was applied, which corresponds to the findings of Rohlmann *et al.* [12] in a study on simulating a standing position in spinal FE models. After acquiring an FE model with adapted bone elements, the biomechanics of the disc were altered to simulate degeneration. As explained in Chapter 2, Section 2.1, degeneration is often described as stiffening of the AF.

The material sensitivity study described in the previous chapter has shown that a bigger C_1 coefficient of the AF ground matrix results in a steeper force/displacement curve, suggesting a stiffer disc. Therefore, disc stiffening was simulated by increasing the AF C_1 coefficient. The first increase was by a factor twenty. This corresponds to $C_1 = 0.436$ which is also the value used by Newell *et al.* [13]. After that, the initial C_1 was increased by a factor thirty, resulting in $C_1 = 0.654$).

4.4. RESULTS

Four FE analyses to assess bone adaptation were performed. The first simulation was to assess maximal principal strains in the model with default material properties for a healthy intervertebral disc where all trabecular elements have been assigned the same initial stiffness. The maximum principal strains in the vertebra were extracted and can be seen in Figure 4.2. This output was then used as input for the bone adaptation algorithm. The algorithm ran iteratively until a desired convergence was reached, meaning that trabecular elements were assigned a Young's Modulus that resulted in an amount of strain within the lazy zone. As mentioned in Chapter 2, disc degeneration can occur in the form of increased stiffness of the AF. Therefore, after configuration of adapted bone, disc degeneration was simulated by adjusting material properties of the AF. The Neo-Hookean material coefficient of the AF ground matrix was increased (from $C_1 = 0.0218$ to $C_1 = 0.436$ [13] and $C_1 = 0.654$) to mimic degeneration and the renewed input file was subjected to the bone adaptation algorithm. A complementing MATLAB script was written to provide visualisation of the ranges in Young's Moduli. The maximum value denoting the highest stiffness (E_{max}) was divided by a factor ten to create a window for these ranges. FEA results were visualised and can be found in Figure 4.3. Figure 4.4 shows the number of elements representing the particular categories, corresponding to the contents of Table 4.1. The Young's Moduli for adapted bone with a healthy disc (AF $C_1 = 0.0218$) were $E_{min} = 2.58$ MPa, $E_{max} = 541$ MPa and an E_{mean} of 218 MPa. The stiffer disc (AF $C_1 = 0.436$) provided elements with $E_{min} = 0.94$ MPa, $E_{max} = 473$ MPa and an E_{mean}

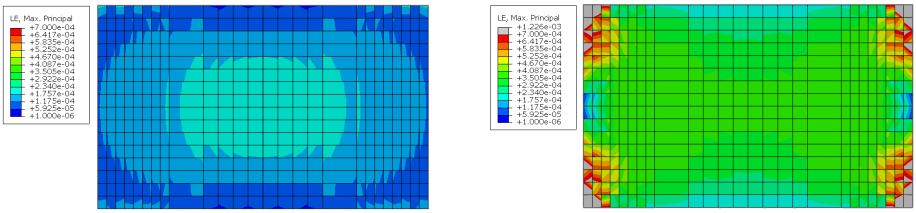

Figure 4.2: Median cut for visualisation of maximum principal strains in a vertebral body before (left) and after (right) bone adaptation as a result from a total uniformly spread load of 500 N.

of 203 MPa. Finally, the stiffest disc (AF C_1 = 0.654) resulted in E_{min} = 1.19 MPa, E_{max} = 394 MPa and an E_{mean} of 192 MPa.

Category	Young's Modulus (MPa)		# of elements		
	From	To	AF C_1 = 0.0218	AF C_1 = 0.436	AF C_1 = 0.654
1	<	54.06	1536	1280	1280
2	54.06	108.12	960	896	960
3	108.12	162.18	0	576	320
4	162.18	216.24	192	192	320
5	216.24	270.3	448	448	384
6	270.3	324.36	144	512	120
7	324.36	378.42	696	1184	904
8	378.42	432.48	256	544	184
9	432.48	486.54	880	0	0
10	486.54	540.6	400	0	0

Table 4.1: Representation of elements categorised over ranges of Young's Modulus

4.5. DISCUSSION

Analysis of the FE model gave several insights in spinal load transmission and vertebral bone adaptation. A few remarks on the results are discussed below.

The average Young's Modulus of trabecular bone (218 MPa, 203 MPa, 192 MPa, respectively) seems to decrease with increasing disc stiffness. Especially the stiffness of the elements in the centre of the vertebral body decreases relative to the outer vertebral elements. Due to continuum modelling, it is unclear whether the trabecular pillars become less stiff or that bone is resorbed in general. In the latter case, this would be confirmed by several studies. For example, Simpson *et al.* [14] performed a histoquantitation study and stated that "[b]one loss was observed in central regions (most distant from the cortex) as [disc] disorganization increased". Accordingly, Twomey and Taylor [15] found that "the loss of the vertical trabeculae is most marked below the [NP]". They describe lumbar vertebrae to become more concave with older age which was also observed by Videman *et al.* [16] (Figure 2.4 in Chapter 2). This change in shape can also be expected

(a) Colour legend for Young's Moduli.

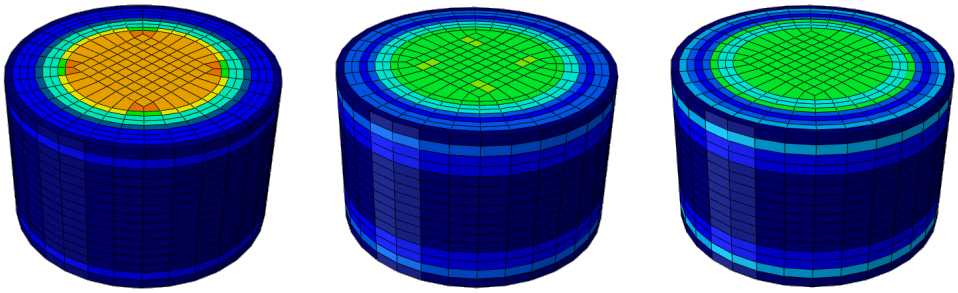

(b) A vertebral body.

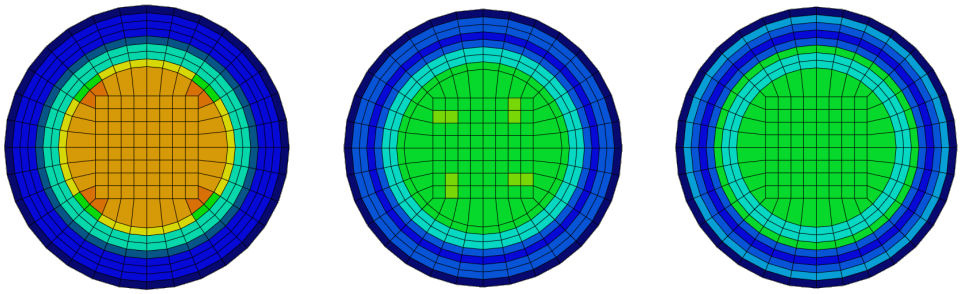

(c) Superior view of a vertebral body.

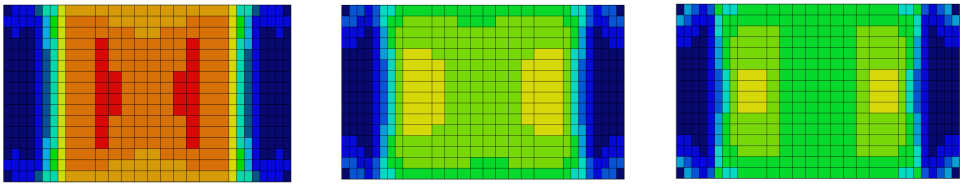

(d) Medial sagittal section of a vertebral body.

Figure 4.3: Visualisation of trabecular bone adaptation after adjusting disc stiffness, AF C_1 = 0.0218, 0.436 and 0.654, respectively

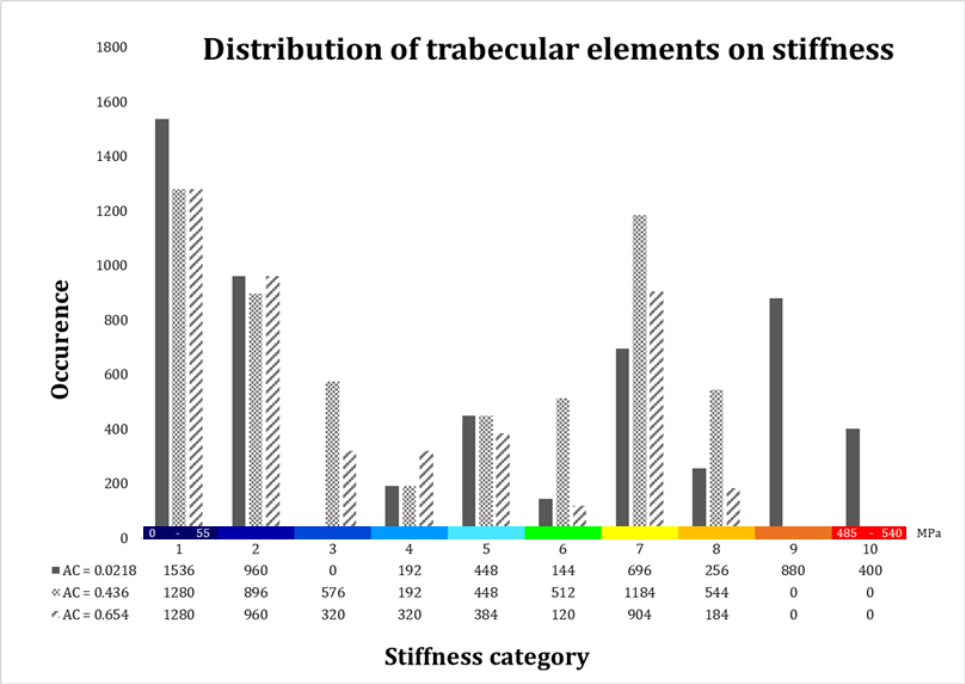

Figure 4.4: Distribution of trabecular bone elements over eleven categories of stiffness. Categorisation details are provided in Table 4.1 and corresponding visualisation of the model can be found in Figure 4.3.

from observing Figure 4.2 which is a visualisation of the maximum principal strains in the vertebral body before and after bone adaptation. This strain pattern becomes even more extreme after disc degeneration, which can be deducted from the change of stiffness in Figures 4.3. The relative Young's Modulus of outer top and bottom outer layers of the body increases as the disc degenerates, suggesting the corners to become stiffer.

The bone adaptation algorithm was designed to adapt both trabecular continuum elements as well as cortical shell elements. However, no adaptation occurred in the latter. The strains in the shell elements were far under the adaption target strain and as a consequence, the shell thickness immediately reached it's lower limit of 0.1 mm. As a reference, an analysis of the vertebra without cortical shells was performed to gain insight in the impact of the cortical bone. Due to the continuum modelling approach, elements could not be iteratively removed from the model but if one assumes the elements with an extremely low Young's Modulus to be fully be resorbed, the results in Figure 4.5 suggest the formation of the aforementioned concave shape. As cortical bone is responsible for 45–75% of the vertebral peak strength [17], leaving out the shell elements would not give accurate insights. Further analyses should be conducted to provide proper simulation of biofidelic shell adaptation.

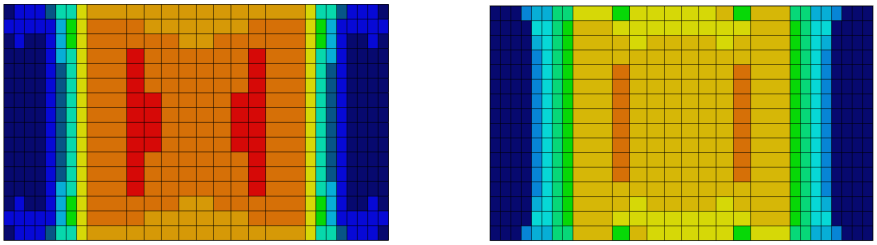

Figure 4.5: Visualisation of trabecular bone adaptation for FE models with (left) and without (right) cortical shell elements. Disc AF C_1 = 0.0218

The elasticity or Young's Modulus of the adapted trabecular bone is quite low compared to values from literature. This can be explained by the fact that trabecular bone, a porous structure, was modelled as continuum elements. Material properties for one element represent the average of both trabecular pillars and voids. Therefore the Young's Modulus of one trabecular element will be lower than the actual Young's Modulus of trabecular bone. The eight stiffer elements in the 'corners' of the NP in the left-hand superior view of the vertebral body (Figure 4.3(c)) are also hypothesised to be the result of average properties. Due to the transition of the square NP centre to its round circumference, these eight elements are smaller than the other elements in the outer NP layer. The latter have a lower Young's Modulus because they are averaged for parts of the NP that are relatively closer to the centre, where elements have lower stiffness.

The next and final Chapter of this thesis contains a summary and conclusion of this project.

REFERENCES

[1] C. Turner, *Three rules for bone adaptation to mechanical stimuli*, Bone **23**, 399 (1998).

[2] D. M. Geraldes and A. T. Phillips, *A comparative study of orthotropic and isotropic bone adaptation in the femur*, International journal for numerical methods in biomedical engineering **30**, 873 (2014).

[3] L. B. Meakin, J. S. Price, and L. E. Lanyon, *The contribution of experimental in vivo models to understanding the mechanisms of adaptation to mechanical loading in bone*, Frontiers in endocrinology **5**, 154 (2014).

[4] A. T. Phillips, C. C. Villette, and L. Modenese, *Femoral bone mesoscale structural architecture prediction using musculoskeletal and finite element modelling*, International Biomechanics **2**, 43 (2015).

[5] H. M. Frost, *The utah paradigm of skeletal physiology: an overview of its insights for bone, cartilage and collagenous tissue organs*, Journal of bone and mineral metabolism **18**, 305 (2000).

[6] Hibbett, Karlsson, and Sorensen, *ABAQUS/standard: User's Manual*, Vol. 1 (Hibbitt, Karlsson & Sorensen, 1998).

[7] I. Mathworks, *Matlab: R2014a*, Mathworks Inc, Natick (2014).

[8] P. S. Foundation, *Python language reference*, Available at http://www.python.org.

[9] D. T. Zaharie and A. T. Phillips, *Pelvic construct prediction of trabecular and cortical bone structural architecture*, Journal of biomechanical engineering **140**, 091001 (2018).

[10] T. M. Keaveny and W. C. Hayes, *A 20-year perspective on the mechanical properties of trabecular bone*, Journal of biomechanical engineering **115**, 534 (1993).

[11] J. Y. Rho, R. B. Ashman, and C. H. Turner, *Young's modulus of trabecular and cortical bone material: ultrasonic and microtensile measurements*, Journal of biomechanics **26**, 111 (1993).

[12] A. Rohlmann, T. Zander, M. Rao, and G. Bergmann, *Applying a follower load delivers realistic results for simulating standing*, Journal of biomechanics **42**, 1520 (2009).

[13] N. Newell, D. Carpanen, G. Girgoriadis, J. Little, and S. Masouros, *Material properties of degenerate and non-degenerate human lumbar intervertebral discs across strain rates*, JMBBM (Under Revision, 2019).

[14] E. Simpson, I. Parkinson, B. Manthey, and N. Fazzalari, *Intervertebral disc disorganization is related to trabecular bone architecture in the lumbar spine*, Journal of Bone and Mineral Research **16**, 681 (2001).

[15] L. Twomey and J. Taylor, *The lumbar spine: structure, function, age changes and physiotherapy*, Australian journal of Physiotherapy **40**, 19 (1994).

[16] T. Videman, M. C. Battié, L. E. Gibbons, and K. Gill, *Aging changes in lumbar discs and vertebrae and their interaction: a 15-year follow-up study*, The Spine Journal **14**, 469 (2014).

[17] S. D. Rockoff, E. Sweet, and J. Bleustein, *The relative contribution of trabecular and cortical bone to the strength of human lumbar vertebrae*, Calcified Tissue Research **3**, 163 (1969).

5

CONCLUSION

This concluding chapter is an elaboration on the scientific relevance of this research's findings. An FE model of a section of the spine was built and validated. An algorithm for bone adaptation was derived from literature and adjusted to the model's geometry and purpose of this project. Analyses were performed according to the principle of the FEM to provide insight in vertebral bone adaptation as a result of altering the biomechanical properties of the intervertebral disc.

5.1. ASSESSMENT OF RESEARCH OBJECTIVES

Five research objectives were formulated in the first chapter of this thesis. The assessment of these objectives is discussed below.

1. ***To build an FE model of a spinal unit.***
A `MATLAB` script was written for the assembly of an input file to be opened in `Abaqus/CAE` for FEA. The input file was scripted to create a model of a part of the spinal column. The geometry of the model was simplified by modelling it as a cylinder. It was sectioned into parts representing two intervertebral discs, consisting of an NP and AF ground matrix with collagen fibres, and adjacent end plates, bilayers of BEPS and CEPS, and vertebrae according to realistic measurements that were derived from literature. In this preliminary and simplified model, the vertebral pedicles and ligaments were not simulated for computational efficiency. Material properties were derived from literature and a material sensitivity test was performed to establish optimisation of those values. An extensive elaboration on the building process of the model is provided in Chapter 3, Section 3.3.

2. ***To comment on the validity of the model.***
The FE model has been validated by means of a material sensitivity study. Experimental data from disc compression tests by Newell *et al.* [1] were used as a reference for the disc's compressional behaviour. After finding that the AF properties had the highest influence on the disc's compressional behaviour, several FE analyses with compression load-

ing were performed on the model for a range of AF material properties. The model's FE force-displacement curve was compared to the average experimental data curve. Based on these outcomes, the best fitting material properties were assigned to the definitive model. Therefore, by ensuring the FEA output to resemble realistic disc behaviour, the model was validated. However, as described in Section 3.6, there are some draws about this method. Firstly, the model was only validated for uniaxial compression within a certain range of compression. The highest compression force that was tested was approximately 1000 N and as one can observe in Figure 3.5, the model's displacement curve diverts from the reference curve for higher compressional forces. It must be noted that the standard deviation of the experimental data for this reference curve also increased with greater compression. Figure 3.6 shows that the model's compressional behaviour still falls well within the ranges found by Newell *et al.* [1]. The validation method of this model was described in Chapter 3, Section 3.6.

3. ***To gain insight in load transmission and the process of bone adaptation as result of disrupted disc biomechanics.***

Strain visualisation of the FEA in Figure 4.3 shows that load is mainly transmitted through outer NP and inner AF layers. In theory, all loads should be transmitted through the AF but it is hypothesised that the stiff shell elements representing cortical bone are preventing this. However, as disc degeneration is simulated by stiffening of the AF, these visualisations indicate that loads are getting transmitted further towards the outer AF layers. Chapter 4, Section 4.4 provides figures indicating altered bone configuration in the vertebral body as a result from changed material properties of the intervertebral disc.

4. ***To approach answering this project's research question using FEA results.***

As stated in the first Chapter, this project's main research question was formulated as:

> *What is the mechanical influence of the intervertebral disc on its adjacent vertebrae?*

Evaluation of the previous research objectives has provided useful information for assessing the project's research question. All observations summarised, the FE analyses have shown that simulation of intervertebral disc degeneration results in adaptation of bone configuration in the adjacent vertebrae. More in detail, the mechanical influence of the intervertebral disc on its adjacent vertebrae can be described as transferring load towards the the area inferior to the AF, relieving the core of the vertebrae of high strains.

5. ***To reflect upon this project's relevance for LBP research.***

Numerous causes of LBP have been reported in literature, of which the vertebrae and end plates are often mentioned. This project's findings indicate that disc biomechanics do indeed influence the adjacent vertebrae. One of the main characteristic results from a degenerated disc is bone resorption of the centre of the vertebral body. As a consequence, the vertebrae lose compressional resistance. This causes both the vertebrae as well as the end plates to become more prone to fracturing. As indicated by Twomey and Taylor [2], bone resorption occurs mostly in the core of the vertebral body and this is explained by Euler's theorem. Bell *et al.* [3] were the first to apply this theorem of a buckling

column to trabeculae: if transverse ties (horizontal trabeculae) are resorbed, the column (vertical trabecula) effectively becomes longer and the buckling load lowers accordingly. This means that with age, the vertebrae become less resistant to loads. They cannot provide strength to support the end plates and consequently, both become more prone to fracturing.

5.2. CONCLUSION

The aim of this research project was to provide an insight into the mechanical influence of the intervertebral disc on its adjacent vertebrae. Visualisation of bone adaptation in combination with a change in disc material properties confirmed the hypothesis that disrupted disc biomechanics indeed affect the adjacent vertebrae. With age, the intervertebral disc becomes stiffer and thus less able to resist compressive loads [4]. Simulations of bone adaptation after inducing this mechanical disruption resulted in a change of trabecular bone material properties which could indicate altering of the internal structures. A loss of bone structure in the centre of the vertebral body would make the vertebra more prone to (micro)fractures which in turn, have been found to be one of many potential causes of LBP [2, 5, 6].

5.3. RECOMMENDATIONS

This goal of this research project was to gain insight into biomechanical influences of the human lumbar intervertebral disc. An FE model was built to assess these influences. However, only uniaxial compressional loading was tested in this research's analyses and consequently, the model was only validated for this loading scheme. In reality, the spine is subjected to various load cases that can all influence the biomechanics of the spinal sections. It is thus recommended to amend the model in such a way that a more extensive set of loading conditions can be applied.

It follows that, if other loading schemes should be tested, the bone adaptation algorithm should be readjusted to orthotropic adaptation rather than the isotropic approach that was used for this project. Geraldes and Phillips [7] showed that their orthotropic algorithm provides a better prediction than an isotropic approach. After optimising and validating the model for other loading conditions, it is therefore advised to adjust the algorithm in a way that it provides a realistic simulation of orthotropic bone adaptation.

As explained earlier, it is hypothesised that the stiff shell elements representing cortical bone are preventing load transmission through the outer AF layers. It might be useful to perform the same simulations without cortical shell elements to confirm this hypothesis and adapt the cortical material properties accordingly.

Furthermore, this model is a coarse approximation of a human intervertebral disc. For example, the cortical shell elements now prevent the vertebrae from forming into their characteristic concave shape. Also, the circular shape of the cylinder may conceal asymmetrical load distribution. Recommendations for further research are therefore to en-

hance the model's geometry.

This project was designed to provide useful insights in potential causes of LBP. In relation to the PhD project of Clement Favier, it suggested to further investigate the effect of observed altered bone configuration on LBP. An example could be to investigate the buckling load of the vertebrae and end plates as a consequence of trabecular alteration. Buckling would indicate (micro)fracturing which can be a source of LBP [5, 6].

REFERENCES

[1] N. Newell, D. Carpanen, G. Girgoriadis, J. Little, and S. Masouros, *Material properties of degenerate and non-degenerate human lumbar intervertebral discs across strain rates,* JMBBM (Under Revision, 2019).

[2] L. Twomey and J. Taylor, *The lumbar spine: structure, function, age changes and physiotherapy,* Australian journal of Physiotherapy **40**, 19 (1994).

[3] G. Bell, O. Dunbar, J. Beck, and A. Gibb, *Variations in strength of vertebrae with age and their relation to osteoporosis,* Calcified tissue research **1**, 75 (1967).

[4] M. A. Adams and P. J. Roughley, *What is intervertebral disc degeneration, and what causes it?* Spine **31**, 2151 (2006).

[5] F. Cecchi, P. Debolini, R. M. Lova, C. Macchi, S. Bandinelli, B. Bartali, F. Lauretani, E. Benvenuti, G. Hicks, and L. Ferrucci, *Epidemiology of back pain in a representative cohort of italian persons 65 years of age and older: the inchianti study,* Spine **31**, 1149 (2006).

[6] H. Sims-Williams, M. Jayson, and H. Baddeley, *Small spinal fractures in back pain patients.* Annals of the rheumatic diseases **37**, 262 (1978).

[7] D. M. Geraldes and A. T. Phillips, *A comparative study of orthotropic and isotropic bone adaptation in the femur,* International journal for numerical methods in biomedical engineering **30**, 873 (2014).

Mechanical Influence of the Intervertebral Disc on the Vertebrae

Eliane Tazelaar
Delft University of Technology

April 2019

Abstract

Background: *To find treatment options for lower back pain, one must gain insight in the spinal anatomy and biomechanics. These can be acquired by using the Finite Element Method. Previously investigated finite element models of the lumbar intervertebral disc have been designed with the main purpose of understanding the biomechanics of the disc itself, and not necessarily its influence on other spinal elements. A change in disc biomechanics is hypothesised to cause a disruption in the surrounding structures such as the vertebrae, which in turn, could result in lower back pain.*

Methods: *A parametric model of a spinal unit was created to be subjected to finite element analyses. The model was validated with experimental data from literature. A bone adaptation algorithm was used to simulate and assess a change in bone material properties before and after simulating disc degeneration by adjusting disc material properties.*

Results: *Finite element analyses showed how a load was transferred by the disc and how bone consequently adapted in response to stiffening the disc properties. The overall trabecular structure was observed to become softer, especially in the vertebral core, while the structure inferior to the Anulus Fibrosus became relatively stiffer.*

Conclusions: *Visualisation of bone adaptation in combination with a change in disc material properties confirmed the hypothesis that disrupted disc biomechanics indeed affect bone configuration in adjacent vertebrae.*

I. Introduction

The human spine enables the human body to move and stand upright by providing axial support and transmitting loads [1]. Lower back pain (LBP) has been defined as "pain and discomfort, localised below the costal margin and above the inferior gluteal folds, with or without leg pain" [2]. In pursuit of finding treatment options, one must gain insight in the spinal anatomy and biomechanics such as joint reaction forces and movement strategies. Toyone et al. [3] carried out MRI studies to investigate correlations between altered vertebral bone-marrow as a result of degenerative intervertebral disc and LBP. Lotz et al. [4] write that degenerating discs are often cause of *annulogenic* pain resulting in LBP [5, 6]. Nevertheless, they state that studies by Fagan et al. [7] investigating innervation of the end plates give evidence that damaged end plates causing *vertebrogenic* pain could also be a major source of LBP. Zhao et al. [8] performed experiments to assess vertebral fractures in end plates and found that in case of failure, this often occurs in cranial before caudal end plates. Several studies report that vertebral microfractures can be a source of back pain [9, 10].

I.1. Elements of the lower spine

The intervertebral disc distributes loads uniformly by resisting spinal compression and simultaneously allowing the spine to bend and twist by permitting (limited) movements of the vertebrae with respect to each other [11]. The Nucleus Pulposus (NP) is the core of the disc and takes up approximately 40-50% of an adult disc's total volume and 29% of the total cross sectional area [12]. The NP has strong osmotic properties that cause the nucleus to swell or shrink by binding to or repelling water, respectively. Swelling due to its high water content generates pressure on the surrounding structures that, in turn, restrict NP swelling in all directions. This mechanism is the source of the disc's ability to withstand compressive forces [13]. The Anulus Fibrosus (AF) is an elastic ring, surrounding and confining the NP by restricting its outward-facing compressive forces resulting from hydrostatic pressure. It consists of several layers (lamellae) of soft

ground matrix (water and solubles), enforced with collagen fibre bundles. The fibres are orientated at an angle of approximately 30° off horizontal and alternate direction per lamella. Neumann [14] write that this specific orientation prevents torsion and vertical separation of the vertebrae while protecting the AF against shear stresses as a result from the tensile stresses that the NP creates. Physical disruption such as changes in tissue properties of the disc can cause degeneration and consequently, altering of the disc's biomechanics [5, 11, 12, 15] and correlations were found between disc degeneration and LBP [16, 17]. Adams et al. [18] describe functional changes as a consequence from disc degeneration. The NP decreases in size and consequently exerts less pressure on the AF. As a consequence, the latter takes on more of the compressional load. Simultaneously, the amount of proteoglycan in the AF decreases and this reduces its compressional strength and increases its stiffness [19].

The end plates are placed between the disc and the vertebral bodies. Literature is disagreeing on whether they should be deemed part of the disc or of the vertebrae [20]. They are described as a bilayer of hyaline cartilage (cartilage end plates, CEPS) and cortical bone (bony end plates, BEPS) and together, they are approximately 0.58 mm thick [12, 21, 22]. Their main function is to balance the a trade-off between providing strength and porosity. On the one hand, they have to support the stiff vertebral bodies and protect them from fracturing and on the other hand, they allow for particle flow to and from the intervertebral disc. The latter is essential as the disc is not vascularised.

The vertebral body is connected to adjacent intervertebral discs through the aforementioned end plates. Vertebrae are made up of an outer dense *cortical* layer that encapsulates the internal bone structure of the *trabecular* core which is made up of bony pillars, trabeculae, and voids. The structural composition of bone is the result of a trade-off between rigidity and mass: it should be strong enough to withstand loads and forces and at the same time use a minimal volume. According to *Wolff's law*, bone structure adapts to (the lack of) mechanical stimuli [23]. The basis for the current *mechanostat* theory of bone adaptation by Frost [24] is "that the most likely loading-derived stimulus for bone cells would be the strains developed in the bone tissue as a result of loading" [25]. Bone mass and architecture remain unchanged under an optimal range of strain, *the lazy zone*, with 1250 ± 250 μstrain as target. In case of strains higher than this target range, bone formation takes places. As result that bone stiffness increases causing the strains to decrease. The reverse is also true: a strain magnitude below the lazy zone results in bone resorption and a decrease in stiffness follows to ensure that optimal strain is re-established.

I.2. The Finite Element Method

The Finite Element Method (FEM) is a means of assessing a large problem by breaking it down into a number of smaller and simpler sub-problems by performing a Finite Element Analysis (FEA). A body is partitioned by creating a mesh that divides it into a finite number of elements and partial differential equations are solved for those separate elements. A common way of partitioning is to divide a body into a finite number of *continuum* elements. The entire body is assessed as one solid *continuum* with every element getting assigned specific material properties. However, not all biological tissues are continuous. For example, trabecular bone is a porous structure comprising of trabecular pillars and voids. Nevertheless, Phillips et al. [26] write that it is quite common to use a continuum mechanics approach for modelling bone and explain that there are three ways of dealing with the issue mentioned before.

The two generally accepted methods are *microscale* and *macroscale* continuum modelling [26]. The first requires the size of one finite element to be smaller than or corresponding to one structural element of bone. In the continuum part, all elements are considered either 'bone' or 'not bone'. Specific material properties are assigned to the 'bone' elements and the 'not bone' elements can be modelled as voids. The second - macroscale - approach deems the entire structure as one continuum and consequently, voids are not modelled. Empirically established material properties are assigned to the elements, to make the entire structure behave as bone. Both of these approaches are the result of a trade-off between accuracy and computational efficiency. The *microscale* approach often uses μMRI or μCT data to create a highly accurate model of bone structure whereas the *macroscale* approach is more of an approximate calculation, heavily relying on empirical data. Nonetheless, due to the large number of elements the *microscale* approach is computationally demanding whereas the *macroscale* approach can perform the calculations in a more efficient manner.

To overcome this trade-off, a *mesoscale* alternative was proposed. Rather than using continuum elements, various structural elements can be adopted to represent the structural nature of bone [26]. For example, truss elements can be used to serve as trabecular bone and shell elements can represent cortical bone. This structural *mesoscale* approach enables the FE model to perform with fewer elements but at the same time ensures the elements to be more appropriate for the structure that they represent. It is considered to reach both *microscale* accuracy as well as *macroscale* computational efficiency. Due to the variety of materials and elements in the spinal elements, a hybrid *mesoscale* approach was selected for the models developed for this project. This approach will ensure the FEA results to be more accurate and computationally efficient than either a *micro-* or *macroscale* modelling method. In an earlier systematic review, a selection of FE models of lumbar discs was found and used for reference [27–35]. All models used a continuum approach for the AF ground matrix. The AF fibres were often structurally modelled as truss, cable or spring elements [27–29, 31, 32, 35], but also as parametrically determined material properties within the AF [30, 34]. Like the AF, the NP was modelled as solid continuum elements. Although Chosa et al. [27] did not report the specific use of elements, they mention using direct input of intradiscal pressure that they derived from literature.

II. Methods

MATLAB version R2014a [36] was used to create an input file of a model of a part of the lumbar spine to be used for finite element analyses in Abaqus/CAE [37]. PYTHON [38] scripts were used to extract output from the FEA results for the iterative process of the bone adaptation algorithm.

Finite Element Model

A mesoscale approach was adopted to create a base FE model, comprising of one spinal unit (one disc, two adjacent halve vertebrae, and inter laying EPS). This base model was used to validate the disc section (Figure 1(b)). As the script was written parametrically, a second model of two spinal units was easily created by stacking two base models on top of each other (Figure 1(a)). This resulted in a model to be used for the bone adaptation algorithm on a full vertebral body. With the purpose of this study being a proof of concept and of increasing computational efficiency, the modelling problem was simplified by creating a cylindrical model without ligaments and vertebral pedicles. The disc consisted of two continuum sections, functioning as the NP and AF. A mesoscale approach was adopted by using structural truss elements (T3D2) to represent the collagen fibre bundles. The trabecular part of a vertebral body was modelled in continuum elements (C3D8H) while the cortical bone and end plates were approached by structural shell elements (S4). Table 1 shows the choice of elements and Figure 1 is a visualisation of the model. The bone, end plates and AF fibres were modelled as elastic materials, describing their behaviour in terms of Young's Modulus (MPa) and Poisson's ratio. The disc's continuum elements (NP and AF ground matrix) were appointed material properties expressed in Neo-Hookean hyperelastic coefficients, C_1 and D, respectively. The latter was set to 0 to account for incompressibility [39].

Tissue	Element type	Abaqus element
Trabecular bone	Solid hexahedral	C3D8H
Cortical bone	Solid shell	S4
CEPS	Solid shell	S4
BEPS	Solid shell	S4
AF Fibres	Truss	T3D2
AF Ground Matrix	Solid hexahedral	C3D8H
NP	Solid hexahedral	C3D8H

Table 1: Element types for all sections

Loading & Boundary Conditions

The model was constrained by fixing the bottom of the column in all directions. Only static uniaxial loading was uniformly applied on the top of the column. For model validation, six loads were tested, ranging from 100 to 1000 N. For the bone adaptation analysis, only one loadcase was tested by applying a uniformly spread uniaxial load of 500 N. This magnitude corresponds to a the force on a disc in a static standing position [40].

Model Validation

Prior to the finite element analyses, material properties were determined by performing a two-fold material sensitivity study. Newell et al. [41] created an FE model of an intervertebral disc and performed *in*

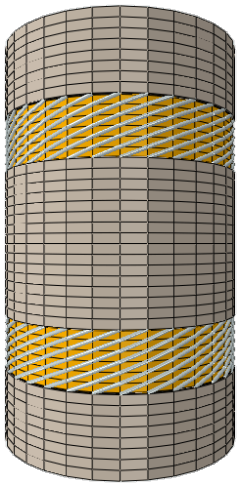

(a) Mesoscale FE model of two spinal units.

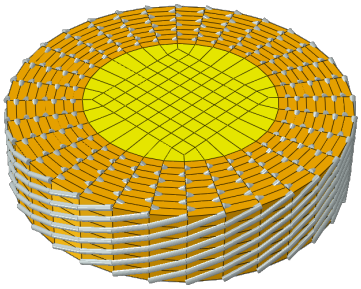

(b) Mesoscale FE model of the intervertebral disc.

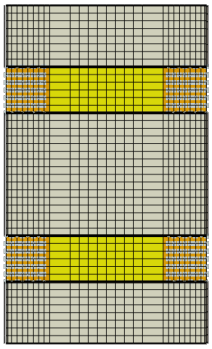

(c) Median sagittal view of two spinal units.

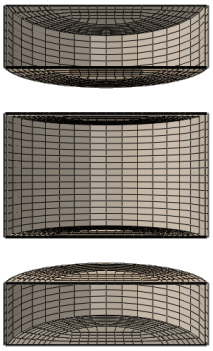

(d) Shell elements representing cortical bone and end plates of two spinal units

Figure 1: Rendered view of the FE model of two spinal units. Yellow: NP, orange: AF ground matrix, White: bone, grey: AF fibres, beige: cortical bone and end plates.

vitro experiments on human lumbar discs to investigate compressional behaviour. Initial material properties from this study were used to investigate which of those properties were most influential for this FE model's compressional behaviour. The second step was to to approach the most fitting values for these influential material properties by comparing output to experimental data. Initial properties from the the FE model by Newell et al. [41] were used and properties were adjusted to ensure model behaviour comparable to the results of said study. This material sensitivity study also served as a means to validate the model.

Tissue	Young's Modulus*	Poisson's ratio	Thickness (mm)
Trabecular bone [42, 43]	10,400	0.3	
Cortical bone [42, 43]	18,600	0.3	
CEPS [44]	23.8	0.4	0.406
BEPS [42, 43]	18,600	0.3	0.174

Table 2: Initial material properties used for material sensitivity study In MPa

Bone Adaptation Algorithm

Geraldes and Phillips [45] proposed an optimisation algorithm for orthotropic bone adaptation in FE models. The algorithm operates by assigning initial material properties to every bone element and extracting the element's internal maximum principal strain values from the iterative FE analyses. These are then used to calculate the absolute maximum strains and consequently approach the true material properties that allow the bone to remain under an optimal target strain. This target is defined as *the lazy zone*, of 1250 $\pm$ 250 μstrain [25]. The iterative process continues until 98 % of the elements reaches that zone and remains unchanged. The bone adaptation algorithm used for this analysis was derived from the study by Zaharie and Phillips [46]. This version of the algorithm was written to approach *orthotropic* bone adaptation. However, to increase computational efficiency and due to the sole use of uniaxial loading, the algorithm was adjusted to simulate *isotropic* adaptation. Therefore, rather than maximum strains for all separate directions, only the absolute maximum principal strain was extracted for each element. Material properties of bone were expressed in Young's Modulus and Poisson's ratio. The latter is often assumed to be 0.3 for bone in structural analyses and was therefore kept constant

[43]. To account for trabecular bone adaptation, Equation 1 shows the iterative calculation for a bone element's Young's modulus (E_i^{it}) by multiplying the modulus of previous iteration with a coefficient calculated from the absolute maximum principal local strain (ε_{max}) that occurs in the element and the target strain (ε_{nt}) [24, 26]. A similar approach was used to model cortical bone adaptation. However, rather than changing the Young's Modulus, the thickness of cortical bone shell elements was iteratively adjusted.

$$E_i^{it} = E_i^{it-1} \frac{|\varepsilon_{max}^{it}|}{\varepsilon_{nt}} \quad (1)$$

The adaptation was first run on the FE model with material properties for a healthy intervertebral disc that were acquired after the material sensitivity study. For this simulation, initial material properties of bone were taken from literature [42, 43] and are summarised in Table 2. After acquiring an FE model with adapted bone elements, the biomechanics of the disc were altered to simulate degeneration. Degeneration is often described as stiffening of the AF. This was simulated by increasing the AF C_1 coefficient with a factor 20 and 30, respectively. As a reference, the first bone adaptation analysis (with a 'healthy' disc) was also performed on a spinal unit without cortical shell elements.

III. Results

Material Sensitivity Study

The AF material properties were found to have the biggest impact on the disc's stiffness. The ground matrix affected the overall stiffness, whereas the fibre's properties changed hyperelastic behaviour into more linearly elastic behaviour. The AF properties were adjusted to ensure the model's compressional behaviour to approach experimental data from Newell et al. [41]. The results of this comparison can be observed in Figure 2. The final properties are displayed in Table 3.

Tissue	Young's Modulus (MPa)	Poisson's ratio
AF Fibres	306.16	0.35
	C_1	D
AF Matrix	0.0218	0
NP	0.00218	0

Table 3: Material properties acquired after material sensitivity study

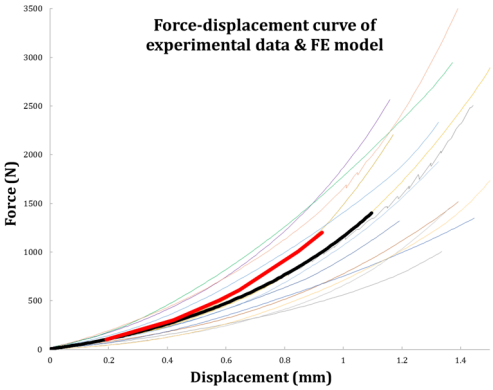

Figure 2: Graphical results of the sensitivity study on FEA material properties.
C1 indicates the first material coefficient of the Neo-Hookean model and FYM stands for the Young's Modulus (MPa) of the AF collagen fibres.

Bone Adaptation

The algorithm resulted in adapted Young's Moduli for the trabecular bone elements. The cortical bone elements, however, immediately decreased in thickness to the lower limit of the algorithm (0.1 mm). The Young's Moduli for adapted bone with a healthy disc (AF C_1 = 0.0218) were E_{min} = 2.58 MPa, E_{max} = 541 MPa and an E_{mean} of 218 MPa. The stiffer disc (AF C_1 = 0.436) resulted in trabecular elements with E_{min} = 0.94 MPa, E_{max} = 473 MPa and an E_{mean} of 203 MPa. Finally, the stiffest disc (AF C_1 = 0.654) gave Young's moduli of E_{min} = 1.19 MPa, E_{max} = 394 MPa and an E_{mean} of 192 MPa. The range of elasticity was divided into ten categories after the FEA with the healthy disc. Figure 5 shows the number of elements representing the particular categories corresponding to the contents of Table 4. As mentioned in the previous section, an additional analysis on a 'healthy' spinal unit *without* cortical shell elements was performed. Figure 3 shows the results from the same analysis for a vertebra with and without shell elements.

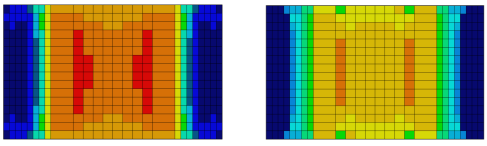

Figure 3: Visualisation of trabecular bone adaptation for FE models with (left) and without (right) cortical shell elements. Disc AF C_1 = 0.0218

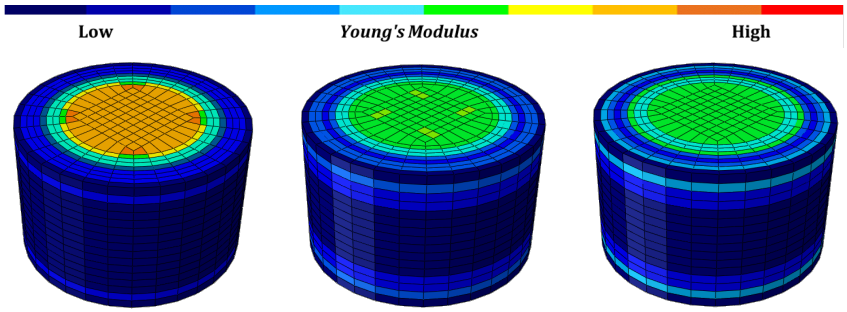

(a) The vertebral body.

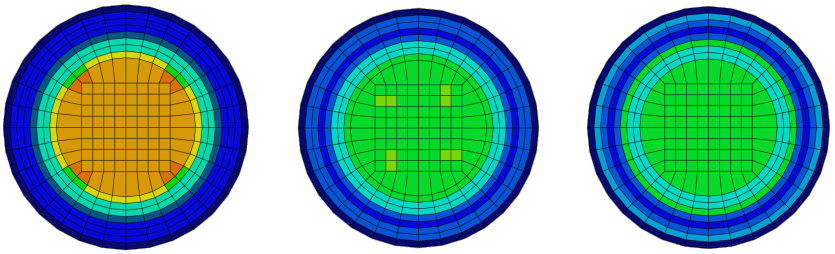

(b) Superior view of the vertebral body.

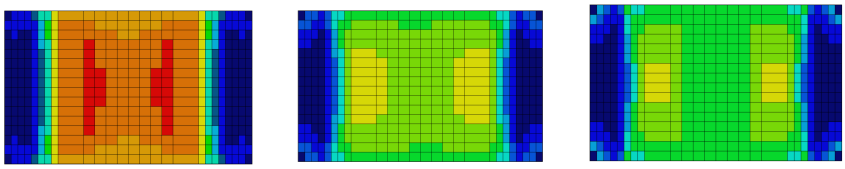

(c) Medial sagittal section of the vertebral body.

Figure 4: Visualisation of trabecular bone adaptation after adjusting disc stiffness, AF C_1 = 0.0218, 0.436 and 0.654, respectively

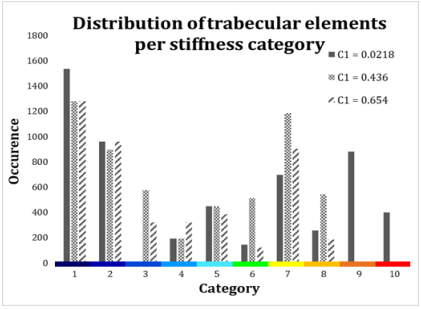

Figure 5: Distribution of trabecular bone elements over eleven categories of stiffness.

	Young's Modulus (MPa)		# of elements		
	From	*To*	*AF C_1:*	*0.0218*	*0.436*	*0.654*
1	<	54.06		1536	1280	1280
2	54.06	108.12		960	896	960
3	108.12	162.18		0	576	320
4	162.18	216.24		192	192	320
5	216.24	270.3		448	448	384
6	270.3	324.36		144	512	120
7	324.36	378.42		696	1184	904
8	378.42	432.48		256	544	184
9	432.48	486.54		880	0	0
10	486.54	540.6		400	0	0

Table 4: Representation of elements divided over ten categories stiffness expressed in Young's Modulus (MPa)

IV. Discussion

Several FE models of intervertebral discs have been developed for various purposes. Most models focused mostly on an accurate and biofidelic representation of the disc, whereas the results of this study's analysis aimed to provide insight the mechanical relation between the disc and its adjacent vertebrae. As this preliminary study is based on results from a simplified model, it should be regarded more as a proof of concept. Further improvements must be made in the model to account for asymmetrical geometry and consequentially, loading and orthotropic adaptation.

As the model could not be validated directly due to difficulty in acquiring *in vivo* experimental data, a two-fold material sensitivity test was performed and served as a validation technique. This validation, however, only made use of experimental data from *in vitro* uniaxial compression tests. Hence, the model has only been validated for this one type of loading. Before performing FEA analysis for other loadcases, the disc model should be revalidated.

The elasticity or Young's Modulus of the adapted trabecular bone is quite low compared to values from literature. This can be explained by the fact that trabecular bone, a porous structure, was modelled by using continuum elements. Material properties for one element represent the average of both trabecular pillars and voids. Therefore the Young's Modulus of one trabecular element will be lower than the actual Young's Modulus of trabecular bone. Additionally, the eight stiffer elements in the 'corners' of the NP in the superior view of the vertebral body with a healthy disc (Figure 4(b)) are also thought to be the result of average properties. Due to the transition of the square NP centre to its round circumference, these eight elements are smaller than the other elements in the outer NP layer. The latter have a lower Young's Modulus because they are averaged for parts of the NP that are relatively closer to the centre, where elements have lower stiffness. Furthermore, the average trabecular Young's Modulus seems to decrease with increasing disc stiffness (218 MPa, 203 MPa, 192 MPa, respectively). Especially the stiffness of the elements in the centre of the vertebral body decreases relatively. Due to the continuum modelling approach, it is uncertain whether the trabecular pillars become less stiff or that bone is resorbed in general. In case of the latter, this would be confirmed by several studies. For example, Simpson et al. [47] performed a histoquantitation study and stated that "[b]one loss was observed in central regions (most distant from the cortex) as [disc] disorganization increased". Accordingly, Twomey and Taylor [48] found that "the loss of the vertical trabeculae is most marked below the [NP]". They describe lumbar vertebrae to become more concave with older age which was also observed by Videman et al. [49] (Figure 6). The relative Young's Modulus of outer top and bottom outer layers of the body increases as the disc degenerates, suggesting that the corner edge become more rigid.

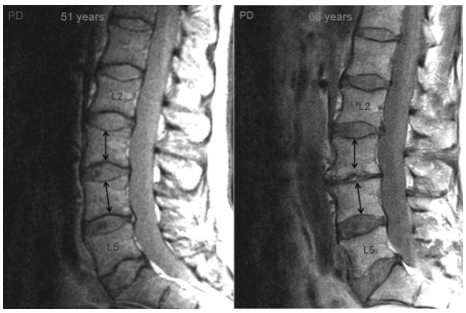

Figure 6: MR images of a 15-year follow-up study on ageing changes in the spine. A collapse of the L3–L4 and height increase in the adjacent vertebrae heights can be observed. Adapted from Videman et al. [49].

The bone adaptation algorithm was designed to adapt both trabecular continuum elements as well as cortical shell elements. Nevertheless, no adaptation occurred in the latter because the strains in the shell elements remained far under the adaption target strain. As a consequence, the shell thickness immediately reached the set lower limit of 0.1 mm. As a reference, an analysis of the vertebra without cortical shells was performed to gain insight in the impact of the cortical bone. Due to the continuum modelling approach, elements could not be iteratively removed from the model but if one assumes the elements with an extremely low Young's Modulus to be fully be resorbed, the results in Figure 3 suggest the formation of the aforementioned concave shape. As cortical bone is responsible for 45–75% of the vertebral peak strength [50], leaving out the shell elements would not give accurate insights. Further analyses should be conducted to provide proper simulation of biofidelic shell adaptation.

V. Conclusion

To the author's knowledge, no FE studies have yet been performed on vertebral bone adaptation as a result from changed disc mechanics. The aim of this preliminary study was to provide an insight in the mechanical influence of the intervertebral disc on its adjacent vertebrae. Visualisation of bone adaptation in combination with a change in disc material properties confirmed the hypothesis that disrupted disc biomechanics indeed affect the adjacent vertebrae. With age, the intervertebral disc becomes stiffer and thus less able to resist compressive loads [11]. Simulations of bone adaptation after inducing this mechanical disruption resulted in a change of trabecular bone material properties which could indicate altering of the internal structures. A loss of bone structure in the centre of the vertebral body would make the vertebra more prone to (micro)fractures which in turn, have been found to be one of many potential causes of LBP [9, 10, 48].

References

[1] Elaine Nicpon Marieb and Katja Hoehn. *Human anatomy & physiology*. Pearson Education, 2007.

[2] Maurits Van Tulder, Annette Becker, Trudy Bekkering, Alan Breen, Maria Teresa Gil del Real, Allen Hutchinson, Bart Koes, Even Laerum, and Antti Malmivaara. Chapter 3 european guidelines for the management of acute nonspecific low back pain in primary care. *European spine journal*, 15:s169–s191, 2006.

[3] T Toyone, K Takahashi, H Kitahara, M Yamagata, M Murakami, and H Moriya. Vertebral bone-marrow changes in degenerative lumbar disc disease. an mri study of 74 patients with low back pain. *The Journal of bone and joint surgery. British volume*, 76(5):757–764, 1994.

[4] JC Lotz, AJ Fields, and EC Liebenberg. The role of the vertebral end plate in low back pain. *Global spine journal*, 3(03):153–164, 2013.

[5] Michael A Adams and Patricia Dolan. Intervertebral disc degeneration: evidence for two distinct phenotypes. *Journal of anatomy*, 221 (6):497–506, 2012. doi: 10.1111/j.1469-7580.2012.01551.x.

[6] Katariina Luoma, Hilkka Riihimäki, Ritva Luukkonen, Raili Raininko, Eira Viikari-Juntura, and Antti Lamminen. Low back pain in relation to lumbar disc degeneration. *Spine*, 25(4):487–492, 2000. doi: 10.1097/00007632-200002150-00016.

[7] Andrew Fagan, Robert Moore, Barrie Vernon Roberts, Peter Blumbergs, and Robert Fraser. Issls prize winner: the innervation of the intervertebral disc: a quantitative analysis. *Spine*, 28(23):2570–2576, 2003.

[8] F-D Zhao, P Pollintine, BD Hole, MA Adams, and P Dolan. Vertebral fractures usually affect the cranial endplate because it is thinner and supported by less-dense trabecular bone. *Bone*, 44(2):372–379, 2009.

[9] Francesca Cecchi, Pierluigi Debolini, Raffaello Molino Lova, Claudio Macchi, Stefania Bandinelli, Benedetta Bartali, Fulvio Lauretani, Enrico Benvenuti, Gregory Hicks, and Luigi Ferrucci. Epidemiology of back pain in a representative cohort of italian persons 65 years of age and older: the inchianti study. *Spine*, 31(10):1149, 2006.

[10] HEATHER Sims-Williams, MI Jayson, and HIRAM Baddeley. Small spinal fractures in back pain patients. *Annals of the rheumatic diseases*, 37(3):262–265, 1978.

[11] Michael A Adams and Peter J Roughley. What is intervertebral disc degeneration, and what causes it? *Spine*, 31(18):2151–2161, 2006. doi: 10.1097/01.brs.0000231761.73859.2c.

[12] N Newell, JP Little, A Christou, MA Adams, CJ Adam, and SD Masouros. Biomechanics of the human intervertebral disc: A review of testing techniques and results. *Journal of the mechanical behavior of biomedical materials*, 69:420–434, 2017. doi: 10.1016/j.jmbbm.2017.01.037.

[13] Keith L Markolf and James M Morris. The structural components of the intervertebral disc: a study of their contributions to the ability of the disc to withstand compressive forces. *JBJS*, 56(4):675–687, 1974. doi: 10.2106/00004623-197456040-00003.

[14] Donald A Neumann. *Kinesiology of the Musculoskeletal System-E-Book: Foundations for Rehabilitation*. Elsevier Health Sciences, 2013.

[15] Stephen J. Ferguson and Thomas Steffen. Biomechanics of the aging spine. *European Spine Journal*, 12(2):S97–S103, Oct 2003. ISSN 1432-0932. doi: 10.1007/s00586-003-0621-0. URL https://doi.org/10.1007/s00586-003-0621-0.

[16] Kenneth MC Cheung, Jaro Karppinen, Danny Chan, Daniel WH Ho, You-Qiang Song, Pak Sham, Kathryn SE Cheah, John CY Leong, and Keith DK Luk. Prevalence and pattern of lumbar magnetic resonance imaging changes in a population study of one thousand forty-three individuals. *Spine*, 34(9):934–940, 2009. doi: 10.1097/BRS.0b013e3181a01b3f.

[17] Evelien IT de Schepper, Jurgen Damen, Joyce BJ van Meurs, Abida Z Ginai, Maria Popham, Albert Hofman, Bart W Koes, and Sita M Bierma-Zeinstra. The association between lumbar disc degeneration and low back pain: the influence of age, gender, and individual radiographic features. *Spine*, 35(5):531–536, 2010. doi: 10.1097/BRS.0b013e3181aa5b33.

[18] MA Adams, DW McMillan, TP Green, and P Dolan. Sustained loading generates stress concentrations in lumbar intervertebral discs. *Spine*, 21(4):434–438, 1996.

[19] Sohei Ebara, James C Iatridis, Lori A Setton, Robert J Foster, Van C Mow, and Mark Weidenbaum. Tensile properties of nondegenerate human lumbar anulus fibrosus. *Spine*, 21(4):452–461, 1996.

[20] Robert J Moore. The vertebral end-plate: what do we know? *European Spine Journal*, 9(2):92–96, 2000.

[21] W Thomas Edwards, Yinggang Zheng, Lisa A Ferrara, and Hansen A Yuan. Structural features and thickness of the vertebral cortex in the thoracolumbar spine. *Spine*, 26(2):218–225, 2001.

[22] S Roberts, IW McCall, J Menage, MJ Haddaway, and SM Eisenstein. Does the thickness of the vertebral subchondral bone reflect the composition of the intervertebral disc? *European Spine Journal*, 6(6):385–389, 1997.

[23] Julius Wolff. *The law of bone remodelling*. Springer Science & Business Media, 2012.

[24] Harold M Frost. The utah paradigm of skeletal physiology: an overview of its insights for bone, cartilage and collagenous tissue organs. *Journal of bone and mineral metabolism*, 18(6):305–316, 2000.

[25] Lee B Meakin, Joanna S Price, and Lance E Lanyon. The contribution of experimental in vivo models to understanding the mechanisms of adaptation to mechanical loading in bone. *Frontiers in endocrinology*, 5:154, 2014.

[26] Andrew TM Phillips, Claire C Villette, and Luca Modenese. Femoral bone mesoscale structural architecture prediction using musculoskeletal and finite element modelling. *International Biomechanics*, 2(1):43–61, 2015.

[27] Etsuo Chosa, Keisuke Goto, Koji Totoribe, and Naoya Tajima. Analysis of the effect of lumbar spine fusion on the superior adjacent intervertebral disk in the presence of disk degeneration, using the three-dimensional finite element method. *Clinical Spine Surgery*, 17 (2):134–139, 2004.

[28] MJ Fagan, S Julian, DJ Siddall, and AM Mohsen. Patient-specific spine models. part 1: Finite element analysis of the lumbar intervertebral disc—a material sensitivity study. *Proceedings of the Institution of Mechanical Engineers, Part H: Journal of Engineering in Medicine*, 216 (5):299–314, 2002.

[29] Fátima Somovilla Gómez, Rubén Lostado Lorza, Marina Corral Bobadilla, and Rubén Escribano García. Improving the process of adjusting the parameters of finite element models of healthy human intervertebral discs by the multi-response surface method. *Materials*, 10(10):1116, 2017.

[30] Nathan T Jacobs, Daniel H Cortes, John M Peloquin, Edward J Vresilovic, and Dawn M Elliott. Validation and application of an intervertebral disc finite element model utilizing independently constructed tissue-level constitutive formulations that are nonlinear, anisotropic, and time-dependent. *Journal of biomechanics*, 47(11): 2540–2546, 2014.

[31] Choon-Ki Lee, Young Eun Kim, Choon-Sung Lee, Young-Mi Hong, Jun-Mo Jung, and Vijay K Goel. Impact response of the intervertebral disc in a finite-element model. *Spine*, 25(19):2431–2439, 2000.

[32] Masao Masni-Azian & Tanaka. Statistical factorial analysis approach for parameter calibration on material nonlinearity of intervertebral disc finite element model. *Computer methods in biomechanics and biomedical engineering*, 20(10):1066–1076, 2017.

[33] Hendrik Schmidt, Fabio Galbusera, Hans-Joachim Wilke, and Aboulfazl Shirazi-Adl. Remedy for fictive negative pressures in biphasic finite element models of the intervertebral disc during unloading. *Computer methods in biomechanics and biomedical engineering*, 14(03):293–303, 2011.

[34] Yvonne Schroeder, Wouter Wilson, Jacques M Huyghe, and Frank PT Baaijens. Osmoviscoelastic finite element model of the intervertebral disc. *European spine journal*, 15(3):361, 2006.

[35] Feng Xie, Honghai Zhou, Wenju Zhao, and Lixin Huang. A comparative study on the mechanical behavior of intervertebral disc using hyperelastic finite element model. *Technology and Health Care*, 25(S1): 177–187, 2017.

[36] Inc Mathworks. Matlab: R2014a. *Mathworks Inc, Natick*, 2014.

[37] Hibbett, Karlsson, and Sorensen. *ABAQUS/standard: User's Manual*, volume 1. Hibbitt, Karlsson & Sorensen, 1998.

[38] Python Software Foundation. Python language reference. Available at http://www.python.org.

[39] Beomkeun Kim, Seong Beom Lee, Jayone Lee, Sehyun Cho, Hyungmin Park, Sanghoon Yeom, and Sung Han Park. A comparison among neo-hookean model, mooney-rivlin model, and ogden model for chloroprene rubber. *International Journal of Precision Engineering and Manufacturing*, 13(5):759–764, 2012.

[40] A Rohlmann, T Zander, M Rao, and G Bergmann. Applying a follower load delivers realistic results for simulating standing. *Journal of biomechanics*, 42(10):1520–1526, 2009.

[41] N Newell, D Carpanen, G Girgoriadis, JP Little, and SD Masouros. Material properties of degenerate and non-degenerate human lumbar intervertebral discs across strain rates. *JMBBM*, Under Revision, 2019.

[42] Jae Young Rho, Richard B Ashman, and Charles H Turner. Young's modulus of trabecular and cortical bone material: ultrasonic and microtensile measurements. *Journal of biomechanics*, 26(2):111–119, 1993.

[43] Tony M Keaveny and Wilson C Hayes. A 20-year perspective on the mechanical properties of trabecular bone. *Journal of biomechanical engineering*, 115(4B):534–542, 1993.

[44] Hiroshi Yamada, F Gaynor Evans, et al. Strength of biological materials. 1970.

[45] Diogo M Geraldes and Andrew TM Phillips. A comparative study of orthotropic and isotropic bone adaptation in the femur. *International journal for numerical methods in biomedical engineering*, 30(9):873–889, 2014.

[46] Dan T Zaharie and Andrew TM Phillips. Pelvic construct prediction of trabecular and cortical bone structural architecture. *Journal of biomechanical engineering*, 140(9):091001, 2018.

[47] EK Simpson, IH Parkinson, B Manthey, and NL Fazzalari. Intervertebral disc disorganization is related to trabecular bone architecture in the lumbar spine. *Journal of Bone and Mineral Research*, 16(4):681–687, 2001.

[48] Lance Twomey and James Taylor. The lumbar spine: structure, function, age changes and physiotherapy. *Australian journal of Physiotherapy*, 40:19–30, 1994.

[49] Tapio Videman, Michele C Battié, Laura E Gibbons, and Kevin Gill. Aging changes in lumbar discs and vertebrae and their interaction: a 15-year follow-up study. *The Spine Journal*, 14(3):469–478, 2014.

[50] S David Rockoff, Edward Sweet, and Jeffrey Bleustein. The relative contribution of trabecular and cortical bone to the strength of human lumbar vertebrae. *Calcified Tissue Research*, 3(1):163–175, 1969.